

**BAŞKENT ÜNİVERSİTESİ**  
**FEN BİLİMLERİ ENSTİTÜSÜ**

131701

**TELSİZ HABERLEŞMESİNDE**  
**UYARLANIR HÜZME ŞEKİLLENDİRME**  
**( ADAPTIVE BEAMFORMING IN**  
**WIRELESS COMMUNICATIONS )**

**Oğuzhan ÇAKIR**

131701

**Yüksek Lisans Tezi**  
**ANKARA**  
**EYLÜL, 2003**

**BAŞKENT ÜNİVERSİTESİ**  
**FEN BİLİMLERİ ENSTİTÜSÜ**

**TELSİZ HABERLEŞMESİNDE**  
**UYARLANIR HÜZME ŞEKİLLENDİRME**

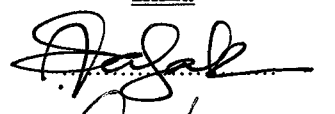
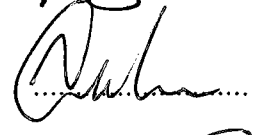
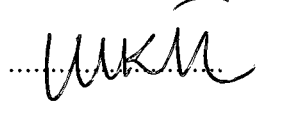
**( ADAPTIVE BEAMFORMING IN**  
**WIRELESS COMMUNICATIONS )**

**Oğuzhan ÇAKIR**

**Yüksek Lisans Tezi**

**ELEKTRİK - ELEKTRONİK MÜHENDİSLİĞİ BÖLÜMÜ**

Bu tez, aşağıda isimleri yazılı jüri üyeleri tarafından 24/09/2003 tarihinde kabul edilmiştir.

<u>Ünvan</u>	<u>Ad - Soyad</u>	<u>İmza</u>
Yrd. Doç. Dr.	Aysel ŞAFAK ( Danışman )	
Prof. Dr.	Turhan ÇİFTÇİBAŞI	
Yrd. Doç. Dr.	Mücahit K. ÜNER	

Onay

8 / 09 / 2003

Prof. Dr. Hüseyin AKÇAY

Fen Bilimleri Enstitüsü Müdürü



# **OUTLINE**

**ÖZ**

**ABSTRACT**

**ACKNOWLEDGEMENTS**

**TABLE OF CONTENTS**

**ABBREVIATIONS**

**LIST OF SYMBOLS**

**LIST OF FIGURES**

**LIST OF TABLES**

1. **ADAPTIVE BEAMFORMING IN WIRELESS COMMUNICATIONS -  
INTRODUCTION**
  2. **WIRELESS COMMUNICATIONS**
  3. **PROPAGATION ASPECTS OF WIRELESS COMMUNICATIONS SYSTEM**
  4. **DIVERSITY AND COMBINING TECHNIQUES**
  5. **ADAPTIVE ANTENNA ARRAYS**
  6. **ADAPTIVE BEAMFORMING**
  7. **ADAPTIVE ALGORITHMS**
  8. **CONCLUSIONS**
- APPENDICES**
- REFERENCES**

## ÖZ

### TELSİZ HABERLEŞMESİNDE UYARLANIR HÜZME ŞEKİLLENDİRME

**Çakır, Oğuzhan**

**Yüksek Lisans Tezi, Elektrik ve Elektronik Mühendisliği Bölümü**

**Tez Yöneticisi: Yrd. Doç. Dr. Aysel ŞAFAK**

**Eylül 2003**

Bu tezde, telsiz haberleşme sistemlerinin başarımları ve kapasitesini arttırmada uyarlanırlar hüzme şekillendirmenin yararları incelenmiştir. Bu çalışmada düzgün lineer dizi (ULA) geometrisine sahip bir uyarlanırlar hüzme şekillendirici kullanılmış ve başarımları bilgisayar simülasyonları ile değerlendirilmiştir. Aynı zamanda en küçük ortalama kareler (LMS), tekrarlayan en küçük kareler (RLS) ve doğrudan örnek kovaryans matrisini tersleyen (DMI) uyarlanırlar dizilerle uyarlanırlar hüzme şekillendirmenin gerçekleştirilebilmesi için gerekli teknikler tanımlanmıştır. Pratik zorlukları bilinen DMI algoritmasının LMS algoritmasından daha hızlı yakınsadığı görülmüştür. DMI algoritması iki temel probleme sahiptir: (1) VLSI'nın kullanımı nedeniyle kolayca üstesinden gelinemeyecek hesaplama karmaşıklığı ve (2) sonlu aritmetik duyarlılık kullanımının ve büyük bir matrisin terslenme gereksiniminin yarattığı sonuçlardaki sayısal kararsızlık. Telsiz haberleşme sistemlerinin başarımları ve kapasitesinde önemli iyileşmeler sağlayan uyarlanırlar diziler ile çeşitleme sistemleri arasında karşılaştırma yapıldı. İstenen ve girişim yapan sinyaller Rayleigh/Rician sönüme uğradığında uyarlanırlar dizilerin başarımlarını saptamada analitik ve bilgisayar simülasyon tekniklerini kullandık. Sonuçlar, uyarlanırlar hüzme şekillendirme yönteminin maksimum oranda birleştirme yönteminden girişimci sayısının anten sayısından daha fazla olduğu durumlarda bile belirgin olarak daha iyi olduğunu göstermektedir. Telsiz haberleşme sistemleri için sonuçlar uyarlanırlar hüzme şekillendirmenin alıcıda sinyal-girişim oranını birkaç desibel arttırdığını göstermektedir. Telsiz haberleşme sistemleri kanal kapasitesinde elde edilen artış

nedeniyle daha büyük frekans tekrarlama aralıđı dolayısıyla daha az sayıda baz istasyon anten gereksinimi duyarlar.

Telsiz haberleşme sistemlerinde uyarlanır hüzme şekillendirme'nin maksimum oranda birleştirme'den daha yüksek başarımlı sağladığı ve daha az sayıda anten gerektirdiđi görülmüştür. Son olarak, telsiz sistemlerinde uyarlanır hüzme şekillendirme'nin LMS, RLS ve DMI uyarlanır dizilerle nasıl gerçekleştirilebileceđi belirtildi. Uyarlanır hüzme şekillendirme'nin sayısal telsiz sistemlerinin kanal kapasitesini ve başarımlını arttırmada öneme sahip olduđu gözlemlendi.

**Anahtar Kelimeler:**

Uyarlanır hüzme şekillendirici, Uyarlanır algoritmalar, Uzaysal-çeşitlenmeli birleştirme teknikleri.



## **ABSTRACT**

### **ADAPTIVE BEAMFORMING IN WIRELESS COMMUNICATIONS**

**Çakır, Oğuzhan**

**M.S., Department of Electrical and Electronics Engineering**

**Supervisor: Asst. Prof. Dr. Aysel ŞAFAK**

**September, 2003**

In this thesis, we have investigated the benefit of the adaptive beamforming approach as a solution to improve the performance and the capacity of the wireless communication systems. In this study, an adaptive beamformer with uniform linear array (ULA) geometry is studied and its performance is evaluated by computer simulations. We also describe techniques for implementing adaptive beamforming with the Least Mean Squares (LMS), Recursive Least Squares (RLS) and, Direct Sample Covariance Matrix Inversion (DMI) adaptive arrays. The DMI approach can be shown to converge more rapidly than the LMS algorithm, the practical difficulties that are associated with the DMI algorithm approach should be appreciated. It has two major problems : (1) increased computational complexity that can not be easily overcome through the use of VLSI, and (2) numerical instability resulting from the use of finite-precision arithmetic and the requirement of inverting a large matrix. A comparison made between the diversity systems and adaptive arrays has shown that a marked improvement in performance and capacity of wireless systems can be obtained. We use analytical and computer simulation techniques to determine the performance of adaptive arrays when the received desired and interfering signals are subject to Rayleigh/Rician fading. Results show that adaptive beamforming schemes is significantly better than maximal ratio combining even when the number of interferers is greater than the number of antennas. Results for wireless systems show that adaptive beamforming increases the output signal-to-interference ratio at the receiver by several decibels. Thus,

systems can require fewer base station antennas and/or achieve increased channel capacity through greater frequency reuse.

With adaptive beamforming schemes the wireless system was seen to have greater margins and requires fewer antennas than with maximal ratio combining. Finally, we described how adaptive beamforming can be implemented in wireless radio with LMS, RLS and, DMI adaptive arrays. Thus, we have shown that adaptive beamforming is a practical means for increasing the channel capacity and performance of digital wireless systems.

**Keywords:**

Adaptive beamformer, Adaptive algorithms, Spatial-diversity combining techniques.



## **ACKNOWLEDGEMENTS**

I'd like to thank to my advisor Asst. Prof. Dr. Aysel Şafak for her motivating and valuable support during this thesis. I also thank to my research assistant colleagues for their contributions.

I also would like to thank to my family for their support and understanding during this thesis work.

I will remember my colleague Sertaç Bahadır with his valuable support.





# TABLE OF CONTENTS

Outline.....	i
Öz.....	ii
Abstract.....	iv
Acknowledgements.....	vi
Table of Contents.....	vii
Abbreviations.....	x
List of Symbols.....	xi
List of Figures.....	xiii
List of Tables.....	xvi
1. ADAPTIVE BEAMFORMING IN WIRELESS COMMUNICATIONS – INTRODUCTION.....	1
2. WIRELESS COMMUNICATIONS.....	4
2.1 THE CELLULAR CONCEPT.....	5
2.2 GEOMETRY OF A HEXAGONAL CELL.....	5
2.3 INTERFERENCE ANALYSIS.....	6
2.3.1 Omnidirectional Antenna System.....	8
2.3.2 Directional Antenna System.....	11
2.3.2.1 Directional Antennas in C=7 Cell Patterns.....	12
2.3.2.2 Directional Antennas in C=4 Cell Patterns.....	13
2.4 INCREASING CAPACITY.....	14
2.5 SPECTRUM EFFICIENCY CONSIDERATIONS.....	14
3. PROPAGATION ASPECTS OF WIRELESS COMMUNICATION SYSTEMS....	18
3.1 RADIO WAVE PROPAGATION.....	18
3.2 SMALL-SCALE MULTIPATH PROPAGATION.....	19
3.3 LARGE-SCALE FADING AND LOGNORMAL SHADOWING.....	20
3.4 PATH LOSS MODEL.....	23

4. DIVERSITY AND COMBINING TECHNIQUES.....	25
4.1 MACROSCOPIC DIVERSITY (Apply on Separated Antenna Sites).....	25
4.2 MICROSCOPIC DIVERSITY (Apply on Co-located Antenna Sites).....	26
4.2.1 Space Diversity.....	26
4.2.2 Frequency Diversity.....	26
4.2.3 Time Diversity.....	26
4.2.4 Polarization Diversity.....	27
4.2.5 Angle Diversity.....	27
4.3 COMBINING TECHNIQUES.....	27
4.3.1 Selection Combining.....	28
4.3.2 Switched Combining.....	28
4.3.3 Maximal Ratio Combining.....	28
4.3.4 Equal-Gain Combining.....	29
4.4 THE EFFECT OF DIVERSITY AND COMBINING TECHNIQUES IN RICIEN FADED AND LOGNORMAL SHADOWED CHANNEL.....	29
4.4.1 Selection Combining.....	29
4.4.1.1 Selection Combining in Rician Fading Channel.....	29
4.4.1.2 Selection Combining in Rician Faded and Lognormal Shadowed Channel.....	31
4.4.2 Maximal Ratio Combining.....	32
4.4.2.1 Maximal Ratio Combining in Rician Fading Channel.....	32
4.4.2.2 Maximal Ratio Combining in Rician-Faded and Log- normal Shadowed Channel.....	33
4.5 COMPUTATIONAL RESULTS.....	33
5. ADAPTIVE ANTENNA ARRAYS.....	39
5.1 LINEAR ARRAY.....	41
5.2 OPERATION OF ADAPTIVE ANTENNA ARRAYS.....	42
5.3 SIMULATION RESULTS.....	44
6. ADAPTIVE BEAMFORMING.....	54
6.1 THE SPATIAL FILTERING PROBLEM.....	55
6.1.1 Statement.....	55
6.1.2 Problem Setup.....	56

6.2 FUNDAMENTALS OF OPERATION.....	56
6.3 MINIMUM MEAN - SQUARE ERROR (MMSE) CRITERIA.....	58
7. ADAPTIVE ALGORITHMS.....	60
7.1 LEAST-MEAN-SQUARE ALGORITHM.....	60
7.2 RECURSIVE LEAST-SQUARES ALGORITHM.....	62
7.3 DIRECT SAMPLE COVARIANCE MATRIX INVERSION.....	63
7.4 SIMULATION RESULTS.....	65
8. CONCLUSIONS.....	75
APPENDICES.....	77
REFERENCES.....	80



## ABBREVIATIONS

AOA	: Angle of Arrival
AWGN	: Additive White Gaussian Noise
BER	: Bit Error Rate
BPSK	: Binary Phase Shift Keying
DMI	: Direct Sample Covariance Matrix Inversion
DPSK	: Non-coherent Differential Phase Shift Keying
EGC	: Equal Gain Combining
LMS	: Least-Mean-Square
LOS	: Line Of Sight
MMSE	: Minimum Mean-Squared-Error
MRC	: Maximal Ratio Combining
MSE	: Mean-Squared-Error
PDF	: Probability Density Function
RLS	: Recursive-Least-Square
SC	: Selection Combining
SINR	: Signal-to-Interference-plus-Noise Ratio
SMI	: Sample Matrix Inversion
SNR	: Signal-to-Noise Ratio
ULA	: Uniform Linear Array

## LIST OF SYMBOLS

$a$	:	path loss exponent for $d \ll g$
$A$	:	offered traffic per cell (erlang / cell)
$A_c$	:	traffic carried by a cell (erlang / cell)
$a_c$	:	traffic carried per channel
$b$	:	additional path loss exponent for $d \gg g$
$B$	:	blocking probability
$C$	:	cluster size
$d$	:	distance between the transmitter and the receiver
$D$	:	distance between two nearest co-channel cells
$E\{.\}$	:	expectation
$E_b / N_0$	:	the ratio of energy per bit to the noise spectral density
$E_s$	:	spectrum efficiency
$g$	:	turning point of the path loss curve
$I_0(.)$	:	modified bessel function of first kind zeroth order
$K_d$	:	Rice factor of the desired signal
$L$	:	number of diversity branches
$m_d$	:	logarithmic mean power of the desired signal
$m_u$	:	logarithmic mean power of the undesired signal
$n$	:	basic propagation path-loss exponent
$N$	:	number of interferers
$N_s$	:	number of channels per cell.
$N_T$	:	total number of available channels
$P_d$	:	received instantaneous power of the desired signal
$P_e$	:	average BER
$P_{od}$	:	local mean power of the desired signal
$P_{0d}'$	:	diffuse component power
$P_{ou}$	:	local mean power of the sum of interfering signals
$P_l$	:	path loss power
$P_r$	:	received power
$P_s$	:	power of LOS component

$P_t$	: transmitted power
$P_n(e n)$	: conditional BER
$R$	: cell radius
$R_u$	: normalized frequency reuse distance
$W$	: bandwidth per channel
$x_{mi}$	: the signal at the output of each of the antenna elements
$\sigma_d$	: shadow spread of the desired signal
$\xi_d$	: area mean signal power of the desired signal
$\xi_u$	: area mean signal power of the sum of interfering signals
$\Gamma$	: interference-to-noise ratio
$\mu$	: number of array elements
$\lambda$	: wave length of the signal



## LIST OF FIGURES

<u>Fig. No</u>	<u>Explanation</u>	<u>Page</u>
2.1	Ideal seven-cell cluster repeat pattern geometry, $D/R=4$ .....	7
2.2	Frequency reuse distance in an idealized hexagonal cell pattern with a cluster of $C= 7$ cells.....	8
2.3	First and second tiers in the cellular system.....	9
2.4	Cochannel interference, worst case in omnidirectional antenna system.....	10
2.5	a) interferers in $120^\circ$ and b) $60^\circ$ sectoring.....	11
2.6	Cochannel interference, worst case in $120^\circ$ sectoring.....	12
2.7	Cochannel interference, worst case in $60^\circ$ sectoring. ....	13
2.8	Cell splitting to increase capacity.....	15
3.1	Typical variation of the received signal power with combined short-term fading and long-term fading.....	21
4.1	Four different diversity combiners.....	30
4.2	Bit error rate for different values of selection combiner over a Rician-faded channel.....	35
4.3	Bit error rate for different values of maximal-ratio combiner over a Rician-faded channel.....	35
4.4	Bit error rate for selection combining ( $L= 1$ ) and several values of Rice-factor $K_d$ over a Rician-faded channel.....	36
4.5	Bit error rate for selection combining ( $L= 2$ ) and several values of Rice-factor $K_d$ over a Rician-faded channel.....	36
4.6	Bit error rate for maximal-ratio combining ( $L= 1$ ) and several values of Rice-factor $K_d$ over a Rician-faded channel.....	37
4.7	Bit error rate for maximal-ratio combining ( $L= 2$ ) and several values of Rice-factor $K_d$ over a Rician-faded channel.....	37
4.8	Comparison of Selection combining and MRC techniques for several values of $L$ .....	38

4.9	Performance comparison improvement of various combining techniques for signal-to-noise ratio SNR and the number of diversity branches $L$ .....	38
5.1	A uniformly spaced linear array ( ULA ).....	41
5.2	Adaptive antenna array.....	43
5.3	Array patterns in rectangular coordinates for several values of $\mu$ with a common element spacing of $d = \lambda/2$ .....	46
5.4	Array patterns in polar coordinates for $\mu=2$ and $\mu=4$ with a common element spacing $d= \lambda/2$ .....	47
5.5	Array patterns in polar coordinates for $\mu=8$ and $\mu=16$ with a common element spacing $d= \lambda/2$ .....	48
5.6	Array patterns in polar coordinates for $\mu=32$ and $\mu=64$ with a common element spacing $d= \lambda/2$ .....	49
5.7	Array patterns in rectangular coordinates for different element spacings with an equal sized aperture of length $10\lambda$ .....	50
5.8	Array patterns in polar coordinates for $d= \lambda/8$ and $d= \lambda/4$ with an equal sized aperture of length $10\lambda$ .....	51
5.9	Array patterns in polar coordinates for $d= \lambda/2$ and $d= \lambda$ with an equal sized aperture of length $10\lambda$ .....	52
5.10	Array patterns in polar coordinates for $d= 2\lambda$ and $d= 4\lambda$ with an equal sized aperture of length $10\lambda$ .....	53
7.1	The average BER against the received SINR for adaptive antennas with one interferer and BPSK modulation. Results are shown for several values of $\mu$ and $\Gamma_1$ .....	67
7.2	The average BER against the received SINR for adaptive antennas with two equal power interferers and BPSK modulation.....	67
7.3	The average BER against the received SINR for adaptive antennas with one interferer and DPSK modulation. Results are shown for several values of $\mu$ and $\Gamma_1$ .....	68
7.4	The average BER against the received SINR for adaptive antennas with two equal power interferers and DPSK modulation.....	68



7.5	The average BER against the received SINR for adaptive antennas with one interferer and NCFSK modulation. Results are shown for several values of $\mu$ and $\Gamma_1$ .....	69
7.6	The average BER against the received SINR for adaptive antennas with two equal power interferers and NCFSK modulation.....	69
7.7	The output MSE of adaptive antenna system for LMS algorithm with varying step size parameter $\alpha$ .....	71
7.8	The output MSE of adaptive antenna system for LMS and RLS algorithms.....	71
7.9	The output MSE of adaptive antenna system for DMI algorithm.....	72
7.10	Array patterns of adaptive antenna system for LMS and RLS algorithms with two interferers, $N = 2$ .....	72
7.11	Array patterns of adaptive antenna system for LMS and DMI algorithms with two interferers, $N = 2$ .....	73
7.12	Array patterns of adaptive antenna system for RLS and DMI algorithms with two interferers, $N = 2$ .....	73
7.13	Array pattern of adaptive antenna system with $\theta_d = 90$ .....	74

## LIST OF TABLES

<b><u>Table No</u></b>	<b><u>Explanation</u></b>	<b><u>Page</u></b>
3.1	Path loss exponents for different environments	23



# **CHAPTER 1**

## **ADAPTIVE BEAMFORMING IN WIRELESS COMMUNICATIONS**

### **INTRODUCTION**

In recent years the growing demand for mobile communication systems, in particular cellular systems has lead to ways of increasing the channel capacity within the allocated spectrum to these services while maintaining satisfactory performance. The transition from analog to digital technology increases the capacity apart from providing efficient handover and channel allocation methods. Specifically, the time division multiple access (TDMA) scheme will result in an improvement over the present analog frequency division multiple access (FDMA) scheme and the broad band code division multiple access (CDMA) scheme expands the capacity over TDMA. These schemes may eventually be limited by the increase in degradation due to interference in the available spectrum. Adaptive antenna arrays have been proposed to reduce multipath fading of desired signal and for cochannel interference suppression, leading to increase in both the performance and the channel capacity. An adaptive antenna array system consists of an array of spatially distributed antennas and the weighting of the received signals optimally so that the output closely approximates a desired signal while minimizing interferences. An array may be used at the base station and/or at the mobile unit, and in both receiving and transmitting mode.

The investigation into the use of adaptive arrays in communications began perhaps more than two decades ago. The objective then was to develop receiving systems for acquiring desired signals in the presence of strong jamming, especially in military communications. Adaptive array systems have been developed for receiving TDMA satellite communications signals and spread spectrum communications signals [5-7].

The use of antenna arrays in mobile radio systems to combat cochannel interference was first discussed by Veh and Reudink in 1980 [8-9]. They showed that with a large number of antenna elements, it was possible to carry out frequency reuse to achieve a very high frequency spectrum efficiency. In an in-depth discussion, they observed that with a moderate number of space diversity branches, much higher spectrum efficiency was achievable, without a spectral penalty, compared to a non-diversity system. A similar concept to that of Yeh and Reudink was independently suggested by Bogachev and Kiselev [10]. They derived the expression for the probability of the probability of the signal-to-interference ratio in the presence of Rayleigh fading. The capability of adaptive arrays and their potential to increase the spectrum efficiency in mobile communications has been gradually recognized by the industry. The analysis given in [11] shows that adaptive beamforming technology allows a reduction in basestation spacing by up to 40 %, thereby increasing the reuse of radio channels by a factor of 2.8. Winters presented an in-depth study of optimum signal combining for space diversity reception in cellular mobile radio systems [12]. In the adaptive beamforming approach, the signals received by the antennas are so weighted and combined that the signal-to-interference-plus-noise ratio (SINR) of the output is maximized, thereby reducing both the effects of Rayleigh fading of the desired signal and the cochannel interference. The results that Winters obtained show that adaptive beamforming is significantly better than maximal ratio combining even when the number of cochannel interferers is greater than the number of antenna elements. Furthermore, adaptive beamforming increases the output SIR at the receiver by several decibels. Since then, the concept of using adaptive antennas in mobile communications has been well received by the communications community.

This study presents an overview of the methods for array beamforming, taking into consideration the recent advances in both direction finding and adaptive beamforming.

This report consists of eight chapters. It is organized as follows. Chapter 2 covers the fundamentals of wireless communications. Interference analysis, omnidirectional and directional antenna systems in cellular communications are discussed. Techniques for increasing capacity in cellular communications are also discussed.

Chapter 3 presents propagation aspects of wireless communications system. It covers radio wave propagation and small-scale multipath propagation. It also covers large-scale fading, lognormal shadowing and path loss model.

In Chapter 4, diversity and combining techniques used in wireless communications are given. Space, frequency, time, polarization and angle diversity techniques are presented. Selection, switched, equal-gain and maximal ratio combining techniques are discussed. The effects of diversity and combining techniques in multipath fading environment and comparison of combining techniques in error performance are also illustrated in this chapter.

Chapter 5 presents adaptive antenna arrays approach for increasing error performance of wireless communications system. Linear array geometry and operation of adaptive antenna arrays are investigated. Some simulation results are also presented.

Chapter 6 gives the fundamentals of adaptive beamforming approach. The solution for the spatial filtering problem in wireless communications and minimum-mean square error (MMSE) criteria is discussed.

In Chapter 7, we present the basic adaptive algorithms used in adaptive beamforming. Least-mean square, recursive least-squares and direct sample covariance matrix inversion algorithms are presented. Comparisons of error performance between maximal ratio combining and adaptive beamforming are illustrated in simulation results section. Comparisons of MSE performance between adaptive algorithms are also illustrated.

Finally, in Chapter 8, some conclusions are presented for the study.

## **CHAPTER 2**

### **WIRELESS COMMUNICATIONS**

Wireless communications has become one of the most rapidly growing industries in the world, and its products are now exerting an impact in all our lives. This is most obvious in the form of the mobile phone; but many other advances, such as digital broadcasting and the wireless internet, will very soon be making their influence felt. In the developing world, wireless communications is also bringing telecommunications to millions who have never yet made a telephone call. In providing different types of wireless services, such as fixed, mobile, outdoor, indoor and satellite communications, the wireless communications industry is experiencing an explosive growth.

Wireless communications have consistently exceeded the capacity of available technology. The exponential increase in voice service, together with the ever-growing demand for data services, have pushed current systems beyond their capacities. There is therefore a continuous pursuit to satisfy these burgeoning demands and for advancing the technological frontiers.

There is a growing need for reliable transmission of high-quality voice and digital data over the terrestrial and satellite-based wireless systems. These systems must be limited in power and spectrum requirements, with the latter prevailing. To lessen the spectrum requirements spectrum and bandwidth-efficient modulation and coding schemes are evolving.

Increasing the capacity of a wireless system, in the presence of limited spectrum, is a never-ending pursuit. Methods have been devised which provide capacity enhancement. The expanding need and explosive growth in wireless communications have led to the development of cellular radio systems. One of many reasons for developing a cellular

radio system is the operational limitation of conventional mobile systems such as limited service capability without hand-off and locating, poor service performance and in sufficient frequency spectrum utilization.

## 2.1 THE CELLULAR CONCEPT

In cellular concept, a desired service area is divided into regions called cells, each with its own land radio equipment for communications with mobile terminals within the cell. A typical cellular radio system consists of three classes of entities: mobile terminals, base station, and mobile switching centers. A mobile terminal contains a control unit, a transceiver, and an antenna system. Each base station has radio equipment and associated control that can provide connection to any mobile terminal located in its cell. The base stations are interconnected and controlled by a central switch. The mobile switching center, the central coordinating element for all base stations, contains a cellular processor and a cellular switch.

## 2.2 GEOMETRY OF A HEXAGONAL CELL

In cellular systems, large planar regions can be covered by two-dimensional networks of small coverage cells. In this system, the cells form a fixed block or cluster around the reference cell in the center and around its cochannel cells. In a cellular system, the minimum number of cells per cluster:  $C$ , in a cell reuse pattern is a function of the cochannel separation. The number of cells per cluster, referred to as *cluster size* as well, is a parameter of major interest, since in practice this number determines how many different channel sets must be formed out of the total allocated spectrum. If the total number of channels available for our system:  $N_T$ , is partitioned into  $C$  cells, then each cell will contain  $N_s = N_T / C$  channels. If one channel set is used in each cell, the telephone traffic demand in some cell will be maximum that cell's  $N_s$  channels. Further growth in traffic within the cell will require a revision of the cell boundaries so that the area formerly regarded as a single cell can now contain several cells and utilize all these cells' channel complements. It is this process which is called cell splitting.

For hexagonal systems, the cluster size:  $C$ , is determined by:

$$C = i^2 + ij + j^2 \quad i, j \geq 0 \quad (2.1)$$

The fact that  $i$  and  $j$  are integers makes geometrically realizable only certain values of the number of cells per cluster, e.g., 1, 3, 4, 7, 9, 12, 13...

$i=2$  and  $j=0$  for  $C=4$ ,  $i=2$  and  $j=1$  for  $C=7$ ,  $i=2$  and  $j=2$  for  $C=12$  ...

Figure 2.1 shows the layout and frequency reuse pattern for a cluster of seven hexagonal cells with  $i=2$  and  $j=1$ . Note that the cochannel cells, i.e., those cells that use the same frequencies, could be located by moving  $i$  cells along any chain of hexagons and turning counter-clockwise  $60^\circ$  and then moving  $j$  cells along the chain. The adjacent cells are allocated different frequencies. Between two cochannel cells many equal size cells must be filled with different frequencies in order to provide a continuity of frequency coverage in space so that the mobile terminals can communicate.

### 2.3 INTERFERENCE ANALYSIS

When customer demand increases, the channels, which are limited in number, have to be repeatedly reused in different areas. This leads to more cochannel cells and increases the system capacity. The minimum separation required between two nearby cochannel cells is based on specifying maximum tolerable cochannel interference due to transmissions from other cochannel cells. The level and distribution of this interference depend on the frequency reuse pattern, the wave propagation phenomenon and the way in which this has been balanced against systems' cost and overall performance objectives.

For a seven-cell cluster, it is noticed from the ensemble of clusters shown in Fig.2.1, that the totality of interference stems from "number 1" cells, which all operate on the same frequency. The base station antennas are assumed to be located at the cell center, and omni-directional antenna pattern are used.



These cells must be separated sufficiently to prevent excessive interference. The ratio of cell separation to cell radius is referred to as the cochannel reuse ratio,  $D/R$ .

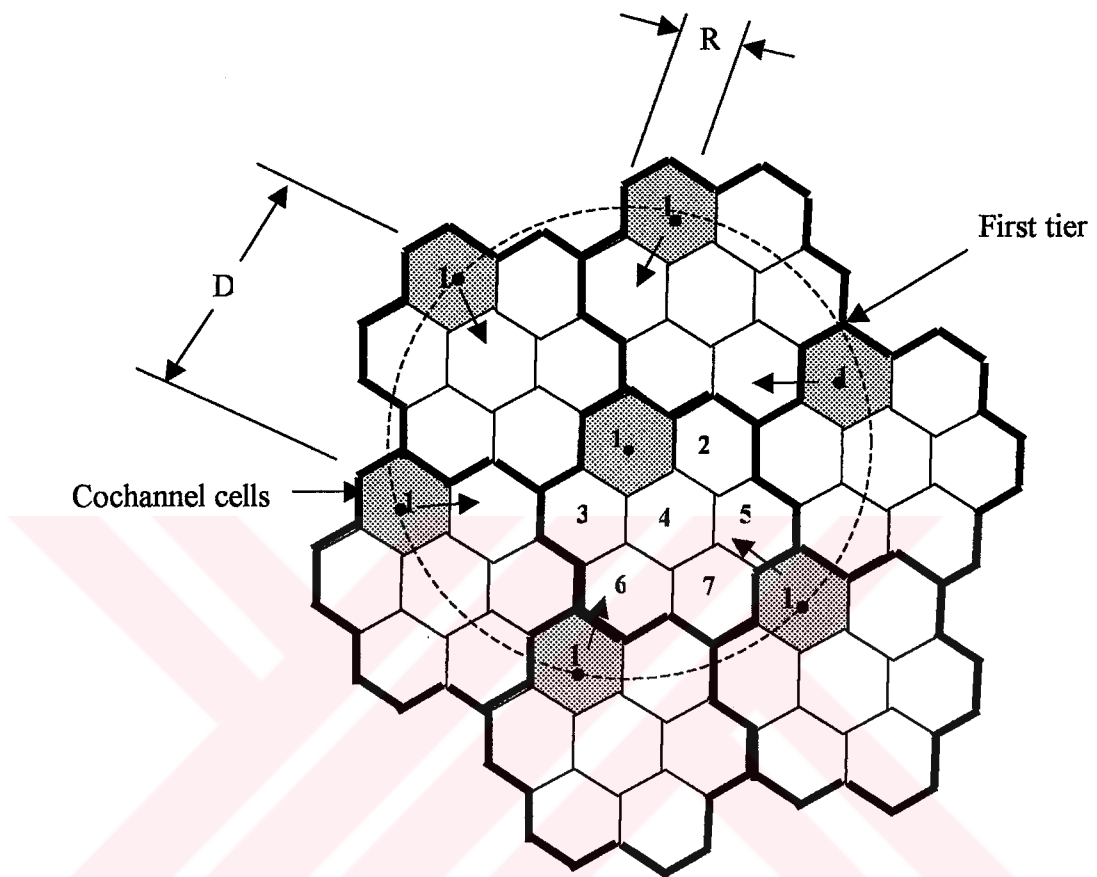


**Figure 2.1** Ideal seven-cell cluster repeat pattern geometry,  $D/R=4.6$

Let  $D$  and  $R$  denote the distance between the centers of two closest cochannel cells, and the radius of the circle approximating the standard cell, respectively. See Figure 2.2.

The *frequency reuse distance* normalized by the cell radius:  $R_u$ , is defined by:

$$R_u = D / R \tag{2.2}$$

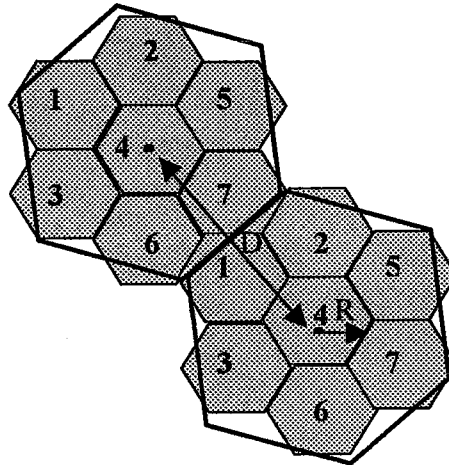


**Figure 2.2** Frequency reuse distance in an idealized hexagonal cell pattern with a cluster of  $C=7$  cells.

For hexagonal systems, the relationship between the normalized frequency reuse distance:  $R_u$ , and the number of cells per cluster:  $C$ , required to completely cover any planar area with a fixed assignment plan is simply:

$$R_u = \sqrt{3C} \quad (2.3)$$

Note that, in view of (2.1),  $R_u$  is allowed to take only some discrete values, as determined by the integer values of the cluster size.

### 2.3.1 Omnidirectional Antenna System

In the start-up phase of a system, omnidirectional antennas are used mainly because of their lower initial cost. In a fully equipped hexagonal shaped cellular system, there are always six cochannel interfering cells in the first tier, as shown in Figure 2.3. The six cochannel interfering cells in the second tier cause weaker interference than those in the first tier. Therefore the cochannel interference from the second tier of interfering cells is negligible.

In the worst case the mobile unit is at the boundary  $R$ , as shown in Figure 2.4. The distances from all six cochannel interfering sites are also shown.

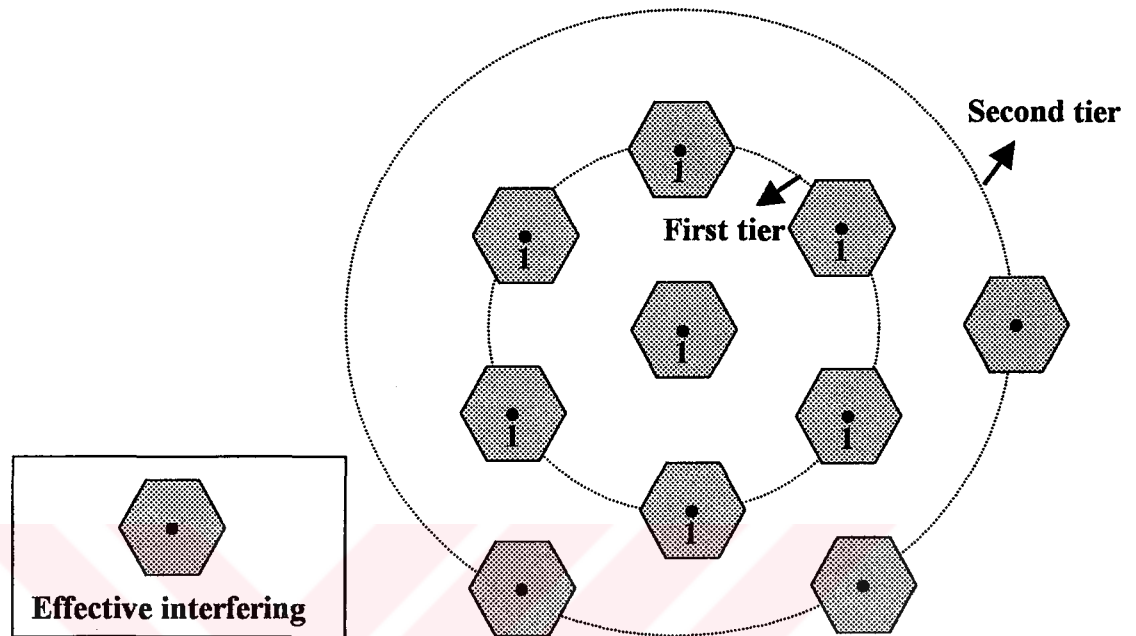


**Figure 2.3** First and second tiers in the cellular system.

The carrier-to-interference power ratio is:

$$\frac{C}{I} = \frac{R^{-4}}{2(D-R)^{-4} + 2D^{-4} + 2(D+R)^{-4}} = \frac{1}{2(R_u - 1)^{-4} + 2R_u^{-4} + 2(R_u + 1)^{-4}} \quad (2.4)$$

To be conservative, we may use the shortest distance  $D-R$  for all six interferers as a worst case, then  $C/I$  ratio is replaced by:

$$\frac{C}{I} = \frac{R^{-4}}{6(D-R)^{-4}} = \frac{1}{6(R_u - 1)^{-4}} \quad (2.5)$$

The minimum distance, which allows the same frequency to be reused, will depend on many factors, such as the number of cochannel cells in the vicinity of the center cell,

the type of geographic terrain contour, the antenna height, and the transmitted power of each base station.

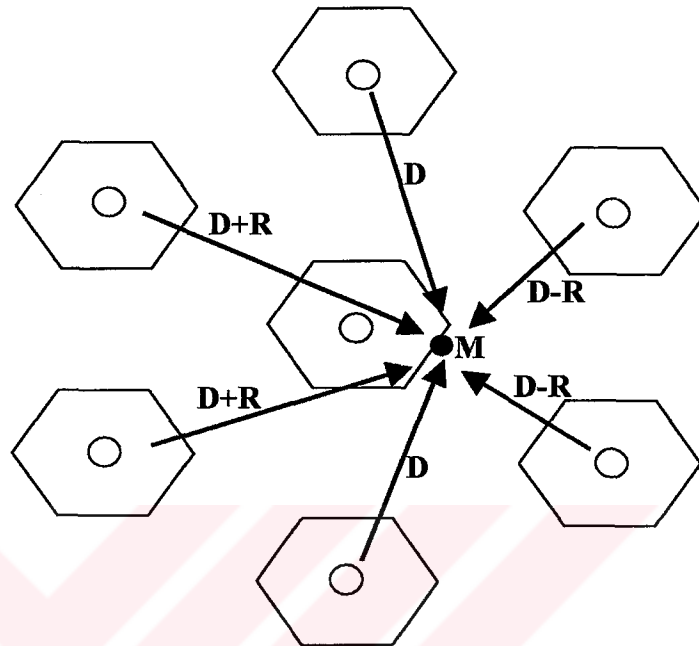


**Figure 2.4** Cochannel interference, worst case in omni directional antenna system.

The reduction of the normalized frequency reuse distance would increase the system capacity and the efficiency of spectrum usage.

If all the base stations transmit the same power, then the cluster size,  $C$ , increases and the frequency reuse distance:  $R_u$  increases. The increased frequency reuse distance reduces the probability of cochannel interference; so a large  $C$  is desired. On the other hand, since the total number of allocated channels:  $N_T$  is fixed, the number of channels assigned to each of  $C$  cells:  $N_s = N_T / C$ , becomes smaller with increasing  $C$ . Therefore, smaller  $C$  provides more channels per cell and per base station. Each base station can thus carry more traffic, thereby reducing the total number of base stations needed for a given total load. The challenge is to obtain the smallest value of cluster size and frequency reuse distance, which can still meet the system performance requirements.

The cluster size, the frequency reuse distance and the number of base stations are limited by several other factors as well, including the economic constraints.

### 2.3.2 Directional Antenna System

In addition to using guard band between the channels and using geographical separation between cochannel cells to reduce interference, the directional antennas could be used to further eliminate the interference. When the traffic begins to increase, the frequency spectrum needs to be used more efficiently and avoid increasing the number of cells per cluster. The cochannel interference may be reduced by using directional antennas which can direct signals into their service area and substantially reduce the interference to the cochannel cells outside their main lobe. Using directional antennas, the PCI can be reduced by more than half since the strong cochannel interference comes from the back cells but not from the front cells. Therefore, directional antenna system can potentially operate with a smaller frequency reuse distance. In these systems, each cell is divided into three or six sectors, thus three or six directional antennas are used at each base station as shown in Figure 2.5.

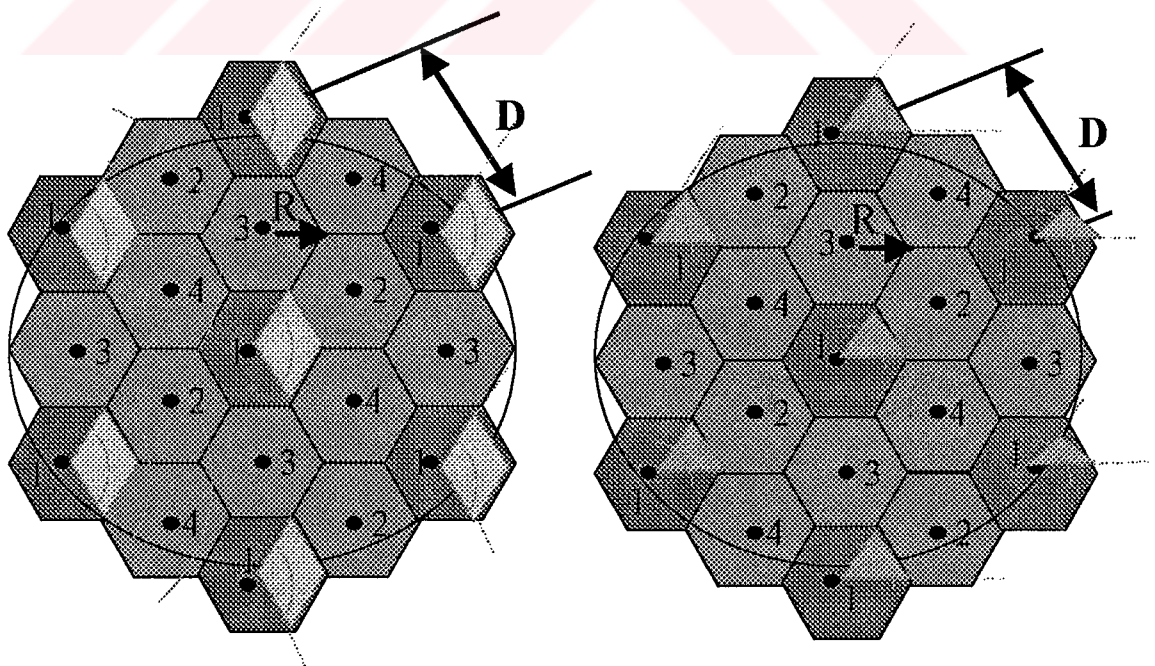


Figure 2.5 a) interferers in  $120^\circ$  and b)  $60^\circ$  sectoring

### 2.3.2.1 Directional Antennas in C=7 Cell Patterns

#### a) Three-sector case

The three-sector case is shown in Figure 2.6. The mobile unit will experience greater interference in the lower shaded cell-sector than in the upper shaded cell-sector. This is because the mobile unit receives the weakest signal from its own cell, but fairly strong interference signal from the interfering cells. In a three-sector case, the interference is effective in only one direction because the front-to-back ratio of a cell-site directional antenna is at least 10 dB or more in a mobile radio environment. Because of the using directional antennas, the number of principal interferers is reduced from six to two. The worst case of C/I occurs when the mobile is at position M, at which point the distance between the mobile unit and the two interfering antennas is roughly  $D + R/2$ . The value C/I can be obtained by the following expression:

$$\frac{C}{I} = \frac{R^{-4}}{(D + 0.7R)^{-4} + D^{-4}} = \frac{1}{(R_u + 0.7)^{-4} + R_u^{-4}} \quad (2.6)$$

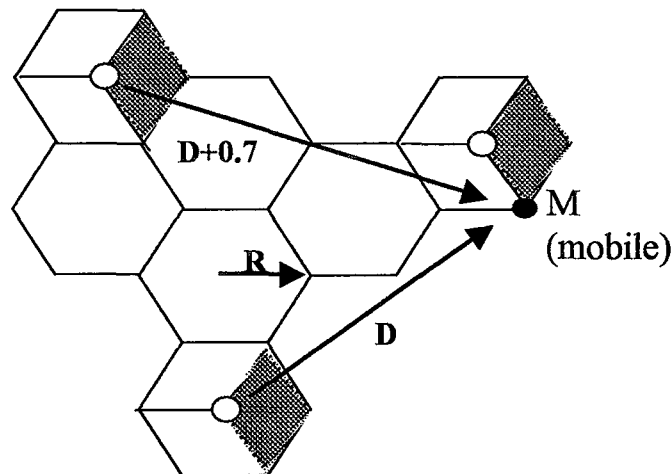


Figure 2.6 Cochannel interference, worst case in 120° sectoring.

### b) Six-sector case

We may also divide a cell into six sectors by using six 60°-beam directional antennas as shown in Figure 2.7. In this case, only one instance of interference can occur in each sector. Therefore, the carrier-to-interference ratio in this case is;

$$\frac{C}{I} = \frac{R^{-4}}{(D + 0.7R)^{-4}} = (R_u + 0.7)^4 \quad (2.7)$$

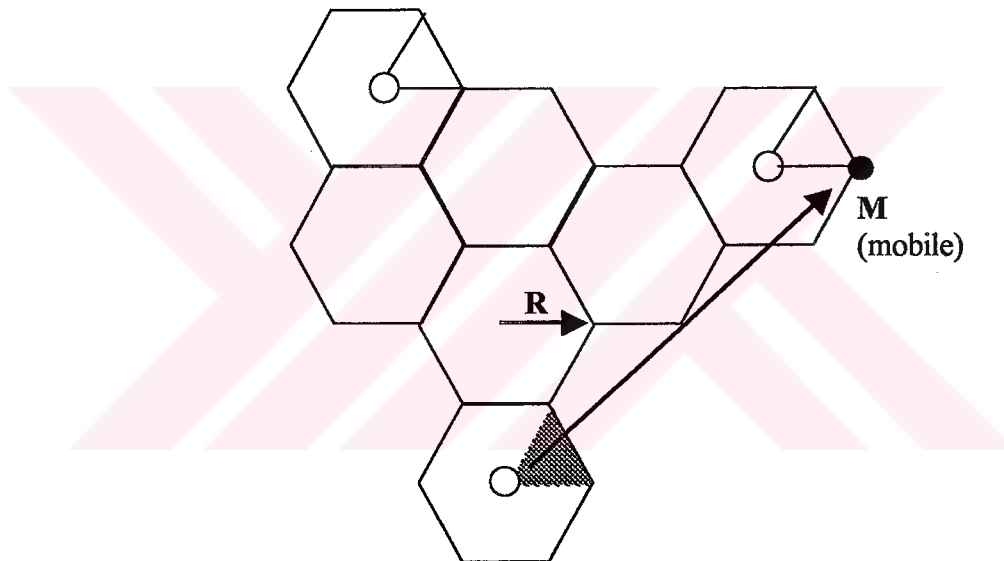


Figure 2.7 Cochannel interference, worst case in 60° sectoring.

### 2.3.2.2 Directional Antennas in C=4 Cell Patterns

#### a) Three-sector case

To obtain the carrier-to-interference ratio, we use the same procedure as in the C=7 cell pattern system. The 120°-beam directional antennas used in the sectors reduced the



interferers to two as in  $C=7$  and  $R_u = \sqrt{(3C)} = 4.6$  systems. For  $C=4$ , the value of  $R_u = \sqrt{(3C)} = 3.46$ .

$$\frac{C}{I} = \frac{1}{(R_u + 0.7)^{-4} + R_u^{-4}} = 20 \text{ dB} \quad (2.8)$$

#### b) Six-sector case

There is only one interferer at a distance of  $D+R$  with  $R_u = 3.46$ , we can obtain

$$\frac{C}{I} = \frac{R^{-4}}{(D+R)^{-4}} = \frac{1}{(R_u + 1)^{-4}} = 27 \text{ dB} \quad (2.9)$$

## 2.4 INCREASING CAPACITY

The techniques of frequency reuse and cell splitting permit a cellular system to meet the important objectives of serving a very large number of customers in a single coverage area while using a relatively small spectrum allocation. When the call traffic in an area increases, the cell is splitted for denser frequency reuse. Cell splitting helps to meet the objective of matching the spatial density of available channels to the spatial density of demand for channels, since lower-demand areas can be served by larger cells with higher-demand areas being served by smaller cells. By decreasing the area of each cell, cell splitting allows the system to adjust to a growing spatial traffic demand density (simultaneous calls per unit area) without any increase in the spectrum allocation.

## 2.5 SPECTRUM EFFICIENCY CONSIDERATIONS

The motivation behind implementing a cellular radio system is to use the available frequency spectrum more efficiently. The techniques of frequency reuse and cell splitting permit a cellular radio system to serve a very large number of customers in a single coverage area while occupying a relatively modest frequency band. If the available channels were distributed among smaller cells, the traffic capacity would be



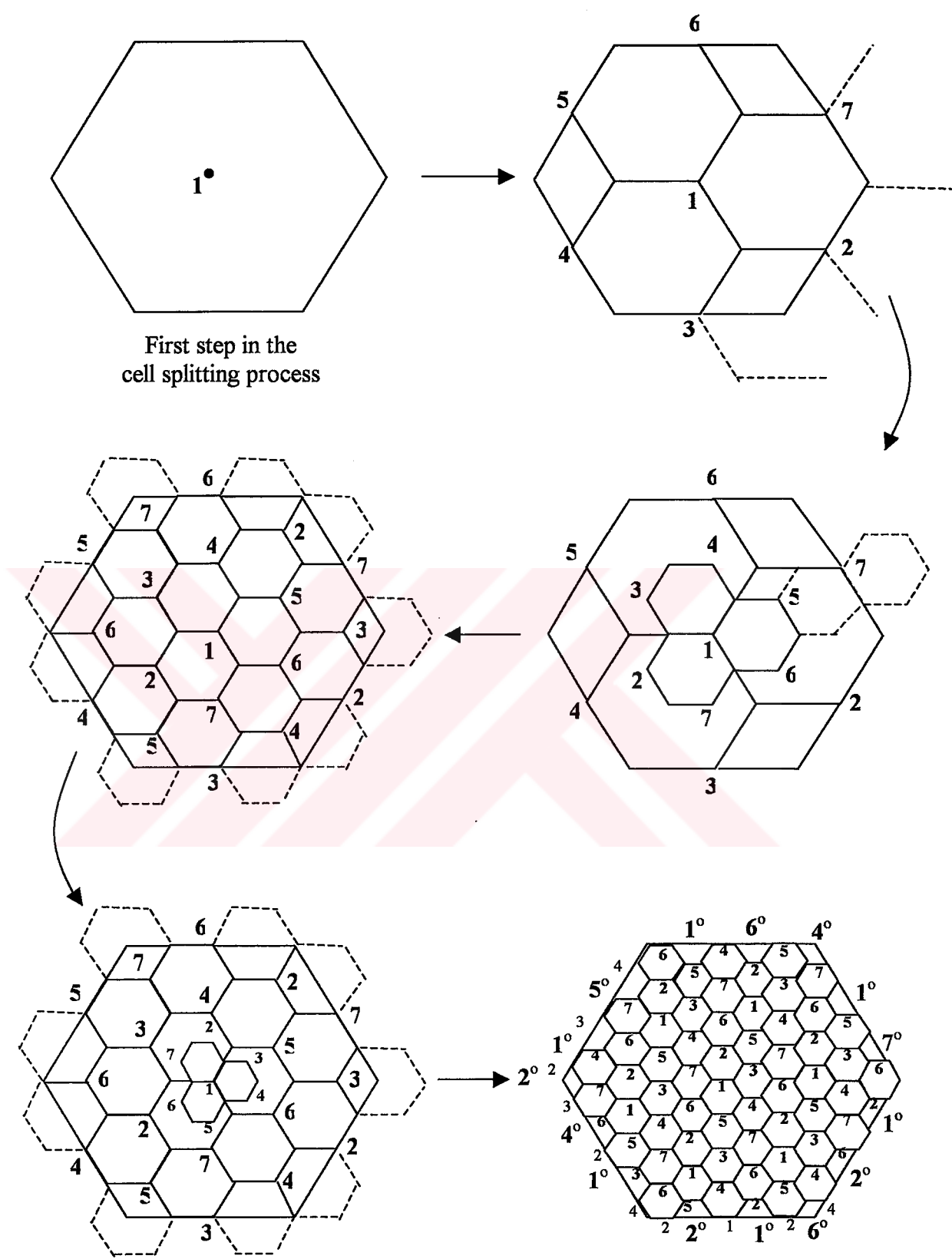


**Figure 2.8** Cell splitting to increase capacity.

greater, while a system with a relatively small capacity would use larger cells. Each channel frequency can then be used for independent calls in several cells, if these are spaced far enough from each other so as to avoid interference. Frequency reuse improves the spectrum efficiency, but at the cost of increasing interference from cochannel cells. The minimum separation required between nearby cochannel cells is based on specifying a maximum tolerable PCI. The level and distribution of PCI depend on the frequency reuse pattern and the wave propagation phenomenon. Future cellular radio systems must be able to operate in the environment of high spectrum congestion and interference. Since the allocated frequency spectrum is limited, this precious resource must be used as efficiently as possible. Therefore one of the principal objectives for the design of cellular radio systems is to maximize the *spectrum efficiency*, which is a measure of the carried traffic per unit bandwidth and per unit cell area. Spectrum efficiency depends on the cellular structure, modulation technique, channel access scheme, correlation between signals and system performance parameters such as an acceptable PCI or call blocking probability.

The techniques for increasing the spectrum efficiency include high-density reuse of the cochannels, narrow band transmission, and demand-assignment multiple access, i.e., efficient time-shared use of the available channels, and increasing the channel efficiency. The capacity of cellular systems is directly related to the spectrum efficiency:  $E_s$ , which is defined by:

$$E_s = \frac{A_c}{N_s W C S_c} \quad \text{erlang/MHz/km}^2 \quad (2.10)$$

Here,  $A_c$  denotes traffic carried by a cell in erlang,  $N_s$  is the number of channels per cell,  $W$  represents bandwidth per channel in MHz,  $C$  is the number of cells per cluster and  $S_c$  the area of a cell in  $\text{km}^2$ . The traffic carried by a cell is given by:

$$A_c = A (1-B) \quad \text{erlang / cell} \quad (2.11)$$

where  $A$  denotes the offered traffic per cell in erlang. The blocking probability:  $B$  is determined using the Erlang-B formula:

$$B = \frac{A^{N_s}}{N_s! \sum_{n=0}^{N_s} \frac{A^n}{n!}} \quad (2.12)$$



## **CHAPTER 3**

### **PROPAGATION ASPECTS OF WIRELESS COMMUNICATIONS SYSTEM**

#### **3.1 RADIO WAVE PROPAGATION**

Signal transmission in wireless communication systems presents significantly different problems other than those encountered in wire-line systems. The channel characteristics are never fixed and vary with movement of the mobile or its surroundings. So the channel is time-variant. These variations require complicated design problems to be solved for securing continued support during a single call, as the terminal moves through the service area. Radio design parameters are chosen to prevent the user as much as possible from experiencing corresponding fluctuations in service quality and reliability.

Apart from the atmospheric effects on the radio waves, the wave propagation may also be influenced by many obstacles such as buildings, hills and even other vehicles between the transmitter and the receiver. So propagation takes place in multipaths. And that is why the instantaneous field strength at the mobile terminal is highly variable. For example radio signals exchanged between a base station and a mobile terminal in a typical urban environment exhibits extreme fluctuations in the amplitude as shown in Figure 3.1.

The prediction of the effect of propagation on system performance parameters is very useful in cellular system design. It can provide information to insure uniform coverage and avoidance of cochannel interference. Moreover, the occurrence of handoff in the cellular system can be predicted more accurately.

### 3.2 SMALL-SCALE MULTIPATH PROPAGATION

Small-scale fading is used to describe the rapid fluctuation of the amplitude of a radio signal over a short period of time or travel distance, so that large-scale path loss effects may be ignored. Fading is caused by interference between two or more versions of the transmitted signal, which arrive at the receiver at slightly different times. These waves, called multipath waves, combine at the receiver antenna to give a resultant signal, which can vary widely in amplitude and phase, depending on the distribution of the intensity and relative propagation time of the waves and the bandwidth of the transmitted signal.

Multipath in the radio channel creates small-scale fading effects. The three most important effects are:

- Rapid changes in signal strength over a small travel distance or time interval.
- Random frequency modulation due to varying Doppler shifts on different multipath signals.
- Time dispersion caused by multipath propagation delays.

In built-up urban areas, fading occurs because the height of the mobile antennas is well below the height of surrounding structures, so there is no single line-of-sight (LOS) path to the base station. Even when a line-of-sight exists, multipath still occurs due to reflections from the ground and surrounding structures. The incoming radio waves arrive from different directions with different propagation delays. The signal received by the mobile at any point in space may consist of a large number of plane waves having randomly distributed amplitudes, phases, and angle of arrival. These multipath components combine vectorially at the receiver antenna, and can cause the signal received by the receiver to distort or fade. Even when the receiver is stationary, the received signal may fade due to movement of surrounding objects in the radio channel.

In the cellular radio environment, the mobile antennas are generally lower than some of the surrounding structures. Consequently, the waves transmitted from or to the base station are often affected by these structures. Reflected, refracted and scattered waves

are generated. Summing all these waves at the receiver antenna results in a fast variation of the received signal. This is called *multipath fading*. The amplitude, phase and angle of arrival (*AOA*) of each of these waves are random variables. Assuming the phase and *AOA* are uniformly distributed, the short-term statistics of the resultant signal envelope fluctuations over local geographic areas approximate a Rayleigh probability density function (pdf). The Rayleigh fading of the mobile radio signals is generally uncorrelated.

The corresponding short-term power (average power measured over a number of RF cycles) of the desired signal,  $P_d$ , is exponentially distributed around the local mean power,  $P_{od}$ :

$$f_{P_d}(P_d | P_{od}) = \frac{1}{P_{od}} e^{-\frac{P_d}{P_{od}}} \quad (3.1)$$

### 3.3 LARGE-SCALE FADING AND LOGNORMAL SHADOWING

In a slow fading channel, the channel impulse response changes at a rate much slower than the transmitted base band signal. In this case, the channel may be assumed to be static over one or several reciprocal bandwidth intervals. In the frequency domain, this implies that the Doppler spread of the channel is much less than the bandwidth of the base band signal. It should be clear that the velocity of the mobile (or velocity of objects in the channel) and the base band signaling determine whether a signal undergoes fast fading or slow fading.

A mobile radio signal envelope is composed of two parts: a fast fading signal and a slow fading (shadowing) signal. The local mean power of the signal can be obtained by smoothing out (averaging) the Rayleigh fading part, and retaining the slow fading part. Shadowing of the mobile radio signal by buildings or hills lead to slow changes in the local mean level, as the mobile terminal moves. The pdf of the local mean signal level is a lognormal distribution. Assuming that the desired and interfering signals are

correlated, the joint pdf of the local mean powers of the desired,  $P_{od}$ , and the sum of interfering signals,  $P_{ou}$ , may be written as:

$$f_{P_{od}, P_{ou}}(P_{od}, P_{ou}) = \frac{e^{-\frac{\tau_d^2 + \tau_u^2 - 2\rho_{d,u}\tau_d\tau_u}{2(1-\rho_{d,u}^2)}}}{2\pi\sigma_d\sigma_u P_{od}P_{ou}\sqrt{1-\rho_{d,u}^2}} \quad (3.2)$$

$$\tau_d = \frac{1}{\sigma_d} \ln\left(\frac{P_{od}}{\xi_d}\right)$$

$$\tau_u = \frac{1}{\sigma_u} \ln\left(\frac{P_{ou}}{\xi_u}\right)$$

Here,  $\sigma_d$ ,  $P_{od}$  and  $\xi_d$  are defined as, respectively; the standard deviation, the local mean power and the area mean power of the desired signal. Similarly,  $\sigma_u$ ,  $P_{ou}$  and  $\xi_u$  stand for, respectively, the standard deviation, the local mean and the area mean power of the sum of interfering signals. The sum of the powers of a finite number of log-normally distributed signals can be approximated, at least as a first order, by another lognormal pdf. Note that  $\rho_{d,u}$  is the correlation coefficient between the desired and the sum of interfering signals.

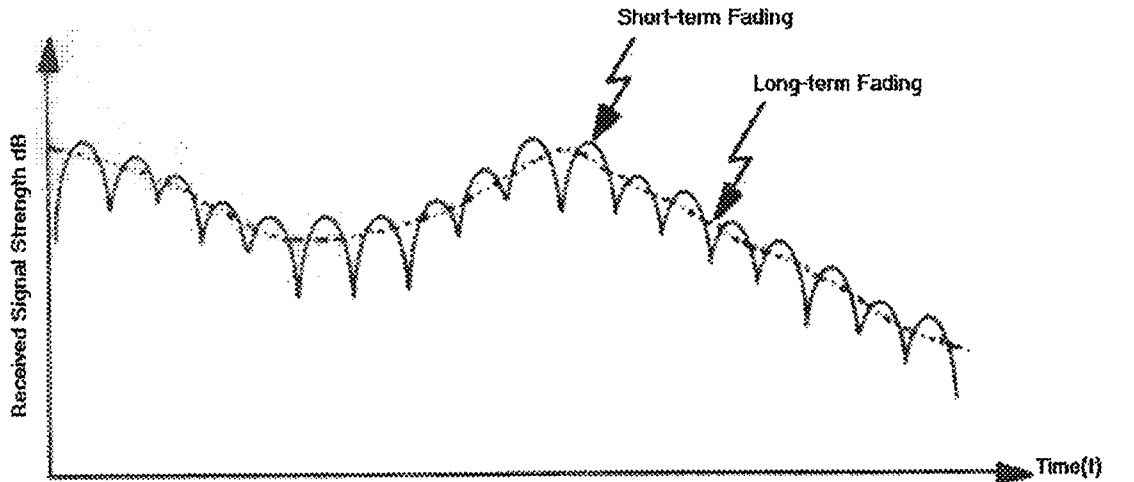


**Figure 3.1** Typical variation of the received signal power with combined short-term fading and long-term fading.

Since the propagation path changes as the mobile terminal moves, the path loss value of a received signal varies over different propagation paths. The path loss fluctuation and the terrain configuration profile at corresponding locations prove to be strongly correlated. Consequently, the local mean powers of the signals whose paths go through the same terrain configurations are also correlated. The received signal is strong when the mobile terminal is at the top of a hill and weak when it is in a valley. The configuration of the terrain affects the standard deviation of the lognormal distribution representing the local mean signal in that area. The standard deviation of the local mean lies between 6-12 dB and with larger standard deviations generally found in more heavily built-up urban areas. Thus the standard deviation is a reflection of how much variation there is in the terrain contour.

Since the obstacles are mostly closer to the mobile terminals, shadowed signals are likely to be correlated in down-links (from base stations to mobile terminals) rather than in up-links (from mobile terminals to base stations). For realistic scenarios in cellular radio systems, the correlation coefficients between the individual signals may vary between 0.4 and 0.6. Nevertheless, these values depend on the angular separation between the directions of arrival and are expected to decrease with increasing angular separation.

In an environment with pure shadowing, the propagation medium is characterized by a joint lognormal pdf of the local mean powers of the desired and the sum of the interfering signals, which are in general correlated. When they are uncorrelated, the joint pdf can be written as the product of lognormal pdf's of the desired and the sum of interfering signals.

In a combined shadowing and fading environment, the short-term power of the cumulative interference is exponentially distributed around the local mean power, which in turn, has a lognormal pdf around the area mean power.



### 3.4 PATH LOSS MODEL

Another important aspect of radio wave propagation between the transmitter and receiver terminal is the prediction of the area mean signal level as a function of range. Both theoretical and measurement-based propagation models indicate that average received signal power decreases logarithmically with distance, whether in outdoor or indoor radio channels. Such models have been used extensively in the literature.

The average large-scale path loss for an arbitrary separation distance between transmitter and receiver is expressed as a function of distance by using a path loss exponent,  $n$ .

$$\bar{P}_r(dB) = \bar{P}_r(d_0) + 10n \log\left(\frac{d}{d_0}\right) \quad (3.3)$$

Where  $n$  is the path loss exponent which indicates the rate at which the path loss increases with distance,  $d_0$  is the close-in reference distance which is determined from measurements close to the transmitter, and  $d$  is the separation distance between transmitter and receiver. The bar in equation denotes the ensemble average of all possible path loss values for a given value of  $d$ . Table 3.1 lists typical path loss exponents obtained in various radio environments.

Environment	Path loss exponent, $n$
Free space	2
Urban area cellular radio	2.7 to 3.5
Shadowed urban cellular radio	3 to 5
In building line-of-sight	1.6 to 1.8
Obstructed in building	4 to 6
Obstructed in factories	2 to 3

**Table 3.1** Path loss exponents for different environments.

The area mean power, around which the local mean power is log-normally distributed, has  $d^{-n}$  type dependence. The distance:  $d$  between the transmitter and receiver system has the path loss exponent  $n$ , which is between 2 and 4. To determine the received powers in terms of the path-loss and the transmitted power levels, we use a dual slope path-loss model, where the received signal power,  $P_r$ , and the transmitted power,  $P_t$ , are related by

$$P_r = \frac{P_t C}{d^a \left(1 + \frac{d}{g}\right)^b} \quad (3.4)$$

Where  $C$  is a constant and  $d$  denotes the distance between the transmitter and the receiver. For  $d \ll g$ , the so-called turning point, the attenuation of the transmitted signal power with distance is given by  $d^{-a}$  ( $a \approx 1.5, 2$ ) while, for  $d \gg g$ , the path-loss is described by  $d^{-(a+b)}$  with  $b \approx 2$ . The path-loss is based on a two-path (direct and earth reflected) propagation model, for which the turning point is given by  $g = 4h_t h_r / \lambda$  ( $h_t$  and  $h_r$  respectively denote the heights of the transmitting and receiving antennas and  $\lambda$  is the wavelength). Empirical data in the UHF band shows that  $g$  lies between 100m and 200m, depending on the antenna heights and the frequency of operation.

## CHAPTER 4

### DIVERSITY AND COMBINING TECHNIQUES

The most adverse propagation effect from which wireless communications systems suffer is multipath fading. Multipath fading, which is usually caused by the destructive superposition of multipath signals reflected from various types of objects in the propagation environments, creates errors in digital transmission. One of the common methods used by the communications community to combat multipath fading is the spatial diversity technique, where two or more antennas at the receiver (or transmitter) are spaced far enough apart that their fading envelopes are uncorrelated.

There are two kinds of fading: Long-term fading (shadowing) and short-term fading. To reduce long-term fading, we need to use macroscopic diversity, and to reduce short-term fading we need to use microscopic diversity.

#### 4.1 MACROSCOPIC DIVERSITY ( Apply on Separated Antenna Sites )

The local mean signal strength varies because of variations of terrain between the transmitter and receiver site. If only one antenna site is used, the traveling mobile unit may not be able to receive the signal at certain geographical locations due to terrain variations such as hills or mountains. Therefore two separated antenna sites can be used to transmit or receive two signals and to combine them to reduce long-term fading. Long-term fading follows a long-normal distribution with a standard deviation whose value depends on terrain variations. The selective combining technique is a recommended technique in the macroscopic diversity scheme since other methods require coherent combining that is difficult to achieve when the receivers are some distance apart. Selective combining means always selecting the strongest from the two fading signals in real time.

## **4.2 MICROSCOPIC DIVERSITY ( Apply on Co-located Antenna Site )**

Multipath fading, which is usually caused by the destructive superposition of multipath signals reflected from various types of objects in the propagation paths. Microscopic diversity is used to reduce the multipath fading. Microscopic diversity uses two or more antennas that are at the same site (colocated) but designed to exploit differences in arriving signals from the receiver. Once the diversity branches are created any of the previous combining methods can be used. Diversity techniques may be classified according to the means by which the additional channels are provided and according to how the multiple signals are combined. The main diversity techniques are called space, time, frequency, polarization and angle diversity.

### **4.2.1 Space Diversity**

Two antennas separated physically by a distance  $d$  can provide two signals with low correlation among their fadings. The separation  $d$  in general varies with the antenna height  $h$  and frequency. The higher the frequency, the closer the two antennas can be to each other. Typically a separation of a few wavelengths is enough to obtain uncorrelated signals.

### **4.2.2 Frequency Diversity**

Signals received on two frequencies, separated by the coherent bandwidth,  $B_c$  are uncorrelated. In order to use frequency diversity in both an urban and a suburban area for cellular and personal communication services frequencies, the frequency separation has to be 300 kHz or greater.

### **4.2.3 Time Diversity**

Time diversity means transmitting identical message in different time slots, which yields two, uncorrelated fading signals at the receiving end. Time diversity is a good scheme for reducing intermodulation at a multi channel site. This system will work for

an environment where the fading occurs independent of the movement of the receiver. In a mobile radio environment, the mobile unit may be at a stand still at any location that has a weak local mean or is caught in a deep fade. Although fading still occurs even the mobile is still, the time-delayed signals are correlated and time diversity will not reduce the fades.

#### **4.2.4 Polarization Diversity**

The horizontal and vertical polarization components,  $E_x$  and  $E_y$ , transmitted by two polarized antennas at the base station and received by two polarized antennas at the mobile unit or vice versa can provide two uncorrelated fading signals. Polarization diversity results in a 3-dB power reduction at the transmitting site due to splitting power into two different polarized antennas.

#### **4.2.5 Angle Diversity**

When the operating frequency is  $\geq 10$  GHz, the scattering of the signals from transmitter to receiver generates received signals from different directions that are uncorrelated with each other. Thus, two or more directional antennas can be pointed in different directions at the receiving site and provide signals for a combiner. This scheme is more effective at the mobile unit than at the base station since the scattering is from local buildings and vegetation and is more pronounced at street level than at the height of base station antennas.

### **4.3 COMBINING TECHNIQUES**

After obtaining the necessary samples, we need to consider the question of processing these samples to obtain the best results. For the most communication systems, the process can be broadly classified as the linear combination of the samples. In the combining process, the various signal inputs are individually weighted and added together.

Since the goal of the combiner is to improve the noise performance of the system, the analysis of combiners is generally performed in terms of SNR. We will examine several different types of combiners and compare their SNR improvements over no diversity.

#### **4.3.1 Selection Combining (SC)**

The algorithm for the selective diversity combining technique is based on the principle of selecting the best signal among all of the signals received from different branches, at the receiving end.

#### **4.3.2 Switched Combining**

Selective combining is an impractical technique for mobile radio communication, a more practical technique known as “Switched Combining”. Assuming that two independent Rayleigh signals  $r_1(t)$  and  $r_2(t)$  are received from two respective diversity branches, the resultant carrier envelope  $r(t)$ , then, can be obtained by using a switch-and-stay strategy. The strategy is to stay with the signal envelope  $r_1(t)$  and  $r_2(t)$  until the envelope drops below a predetermined switching threshold  $A$ , and then to switch to the stronger of two signals. The switched-combined signal always performs worse than the selectively combined signal, except at the threshold level, where performance is equal.

#### **4.3.3 Maximal Ratio Combining**

With maximal-ratio combining (MRC), the diversity branches must be weighted by their respective complex fading gains and combined and maximal-ratio combining results in an ML receiver gives the best possible performance among the diversity combining techniques. In maximal-ratio combining, signals are weighted for optimum performance and are co phased before being combined. In predetection maximal-ratio combining, each signal is co phased at the IF level. The maximal-ratio combining technique can also be applied during post detection of the received signal; a gain control is required following each detection.

#### **4.3.4 Equal-Gain Combining (EGC)**

The maximal-ratio predetection combining technique is an ideal linear diversity-combining technique; however, it requires costly design in receiver circuitry to achieve the correct weighting factors. The selective combining technique selects the strongest signal branch at any given instant of time, but it is also difficult to implement. The switched-combined diversity scheme always provides worse performance than the selective combining diversity scheme. In comparison, equal-gain combining uses a simple phase-locked summing circuit to sum all of the individual signal branches. The equal-gain combining technique still provides incoherent summing of the various noise elements, but it also provides the required coherent summing of all the individual signal branches. Comparing the performance of the equal-gain combiner with that of the maximal-ratio combiner reveals that equal-gain combiner performance is slightly worse than the performance of the maximal-ratio combiner.

#### **4.4 THE EFFECT OF DIVERSITY AND COMBINING TECHNIQUES IN RICIAN FADED AND LOGNORMAL SHADOWED CHANNEL**

In this section two combining techniques are considered, namely selection combining and maximal-ratio combining.

##### **4.4.1 Selection Combining**

Selection combining consists of selecting the antenna supporting the highest base band signal to noise ratio  $S/N$  to be connected to the output.

##### **4.4.1.1 Selection Combining in Rician Fading Channel**

In a Rician fading environment, the amplitude of the received signal has a Rician probability density function. The Rician PDF with selection combining is given below.

$$f(P_d) = L \left[ 1 - Q \left( \sqrt{\frac{2P_{sd}}{P'_{od}}}, \sqrt{\frac{2P_d}{P'_{od}}} \right) \right]^{L-1} \cdot \frac{1}{P'_{od}} \exp \left( -\frac{P_d + P_{sd}}{P'_{od}} \right) I_0 \left( \frac{2\sqrt{P_d P_{sd}}}{P'_{od}} \right) \quad (4.1)$$

where

$$K_d = \frac{P_{sd}}{P'_{od}} = \frac{\text{power in LOS component}}{\text{power in multipath component}}$$

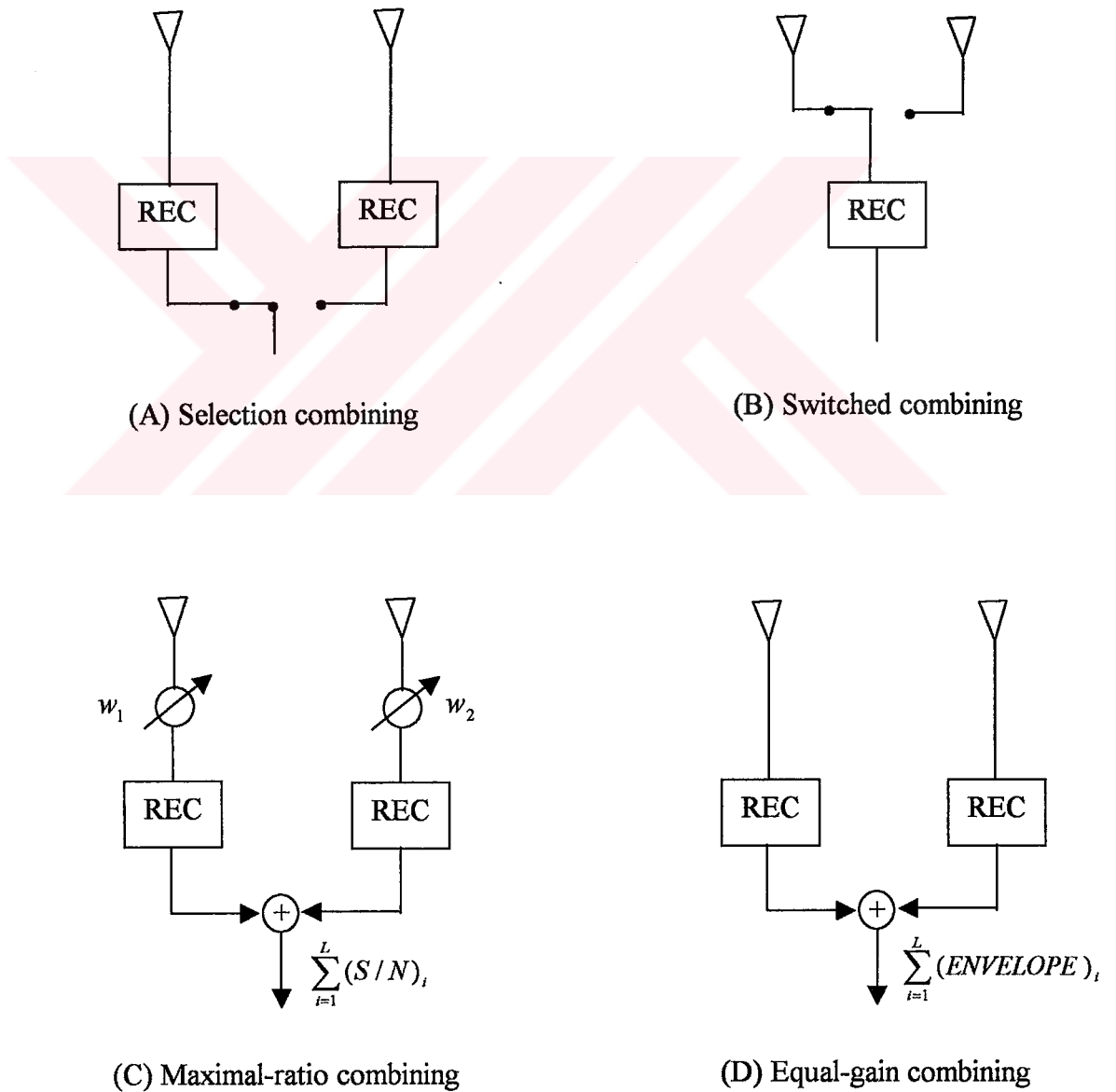


**Figure 4.1** Four different diversity combiners.



For Rice Factor  $K_d = 0$ , (3.1) reduces to a Rayleigh PDF. The case of  $K_d = \infty$  represents a situation with no fading component.  $L$  is the order of diversity and  $Q(a, b)$  is the Marcum Q function which is defined as

$$Q(a, b) = \int_b^{\infty} x \exp\left(-\left(\frac{x^2 + a^2}{2}\right)\right) I_0(ax) dx$$

where  $I_0(\cdot)$  is the modified Bessel function of the first kind and order zero.

The probability of error for non-coherent DPSK ( $A = B = 1$ ) and BPSK ( $A = B = 2$ ) can be expressed as follows. In Appendix A, we have evaluated the probability of error in cellular radio systems.

$$P_e = \int_0^{\infty} \frac{1}{2} \exp\left(-\frac{P_d T_b}{AP_{ou} T_b + BN_0}\right) L \left[ 1 - Q\left(\sqrt{\frac{2P_{sd}}{P'_{od}}}, \sqrt{\frac{2P_d}{P'_{od}}}\right) \right]^{L-1} \cdot \frac{1}{P'_{od}} \exp\left(-\frac{P_d + P_{sd}}{P'_{od}}\right) I_0\left(\frac{2\sqrt{P_d P_{sd}}}{P'_{od}}\right) dP_d \quad (4.2)$$

#### 4.4.1.2 Selection Combining in Rician Faded and Lognormal Shadowed Channel

The probability of density function (pdf) of combined Rician-faded and log normal shadowed channel can be written as;

$$f(P_d) = \int_0^{\infty} \frac{1}{P'_{od}} \exp\left(-\frac{P_d + P_{sd}}{P'_{od}}\right) I_0\left(\frac{2\sqrt{P_d P_{sd}}}{P'_{od}}\right) \frac{\exp\left(-\frac{[\ln P_{sd} - m_{sd}]^2}{2\sigma_{sd}^2}\right)}{\sqrt{2\pi}\sigma_{sd} P_{sd}} dP_{sd} \quad (4.3)$$

The probability of error for non-coherent DPSK ( $A = B = 1$ ) and BPSK ( $A = B = 2$ ) with selection combining in a Rician-faded and lognormal shadowed channel is given below.

$$P_e = \int_0^{\infty} \frac{1}{2} \exp\left(-\frac{P_d T_b}{AP_{ou} T_b + BN_0}\right) L \left[ \int_0^{P_d} f(P_d) dP_d \right]^{L-1} f(P_d) dP_d \quad (4.4)$$

#### 4.4.2 Maximal Ratio Combining

In this method, the L signals are weighted proportionately to their signal to noise power ratios (SNR) and then summed. The individual signals must be co phased before combining, in contrast to selection combining. Maximal-ratio combining (MRC) results in an ML receiver give the best possible performance among the diversity combining techniques.

##### 4.4.2.1 Maximal Ratio Combining in Rician Fading Channel

In a Rician fading environment, the amplitude of the received signal has a Rician probability density function. The Rician pdf with maximal ratio combining can be expressed as;

$$f(P_d) = \frac{1}{P'_{od}} \left( \frac{P_d}{LP_{sd}} \right)^{L-1} \exp\left(-\frac{P_d + LP_{sd}}{P'_{od}}\right) I_{L-1} \left( 2 \sqrt{\frac{LP_d P_{sd}}{P'_{od}}} \right) \quad (4.5)$$

The probability of error for non-coherent DPSK ( $A = B = 1$ ) and BPSK ( $A = B = 2$ ) with maximal-ratio combining in Rician fading channel is as follows

$$P_e = \int_0^{\infty} \frac{1}{2} \exp\left(-\frac{P_d T_b}{AP_{ou} T_b + BN_0}\right) \left[ \frac{1}{P'_{od}} \left( \frac{P_d}{LP_{sd}} \right)^{L-1} \exp\left(-\frac{P_d + LP_{sd}}{P'_{od}}\right) I_{L-1} \left( \frac{2\sqrt{LP_d P_{sd}}}{P'_{od}} \right) \right] dP_d \quad (4.6)$$

#### 4.4.2.2 Maximal Ratio Combining in Rician Faded and Log-normal Shadowed Channel

The pdf for maximal-ratio combining in a shadowed Rician-faded channel can be expressed as

$$f(P_d) = \int_0^{\infty} \frac{1}{P'_{od}} \left( \frac{P_d}{LP_{sd}} \right)^{\frac{L-1}{2}} \exp\left(-\frac{P_d + LP_{sd}}{P'_{od}}\right) I_{L-1}\left(\frac{2\sqrt{LP_d P_{sd}}}{P'_{od}}\right) \frac{\exp\left(-\frac{[\ln(P_{sd}) - LP_{sd}]^2}{2\sigma_{sd}^2}\right)}{\sqrt{2\pi}\sigma_{sd} P_{sd}} dP_{sd} \quad (4.7)$$

The probability of error for non-coherent DPSK ( $A = B = 1$ ) and BPSK ( $A = B = 2$ ) with maximal-ratio combining in a shadowed Rician-faded channel is given below,

$$P_e = \int_0^{\infty} \frac{1}{2} \exp\left(-\frac{P_d T_b}{AP_{ou} T_b + BN_0}\right) f(P_d) dP_d \quad (4.8)$$

### 4.5 COMPUTATIONAL RESULTS

In this section, some computational results related with diversity combining techniques will be presented.

In Figure 4.2, Bit error rate (BER) against SNR is shown for selection combining technique over a Rician-faded channel. Selection combining is seen to give a very large improvement in error performance. The largest diversity gain is achieved with 2-branch diversity and diminishing returns are realized with increasing L.

In Figure 4.3, Bit error rate against SNR is shown for maximal-ratio combining method over a Rician-faded channel. Maximal ratio combining is seen to give larger

improvement than selection combining in error performance. Again, the largest diversity gain is achieved with 2-branch diversity and diminishing returns are realized.

In Figure 4.4 and Figure 4.5, Bit error rate against SNR is shown for selection combining technique over a Rayleigh / Rician-faded channel  $L=1$  and  $L=2$  respectively. Note that the fade distribution will affect the diversity gain. In general, the relative advantage of diversity is greater for Rayleigh fading than Rician fading, because as the Rice factor  $K_d$  increases there is less difference between the instantaneous received signal-to-noise ratios on the various diversity branches. However, the performance will always be better with Rician fading than with Rayleigh fading, for a given average received signal-to-noise ratio and diversity order.

In Figure 4.6 and Figure 4.7, Bit error rate against SNR is shown for maximal ratio combining technique over a Rayleigh / Rician faded channel  $L=1$  and  $L=2$  respectively. Maximal ratio combining is seen to give larger improvement than selection combining in error performance. Again, the relative advantage of diversity is greater for Rayleigh fading than Rician fading.

In Figure 4.8, Cumulative distribution function (CDF) of output SNR against SNR is shown for selection combining and maximal ratio combining techniques. Observe that maximal ratio combining always performs better than selection combining.

In Figure 4.9, performance comparison improvement of various combining techniques is shown for signal-to-noise ratio (SNR) and the number of diversity branches  $L$ . It is apparent that selection combining results in the worst performance, followed by equal-gain. Once again, maximal ratio combining is seen to give best performance.

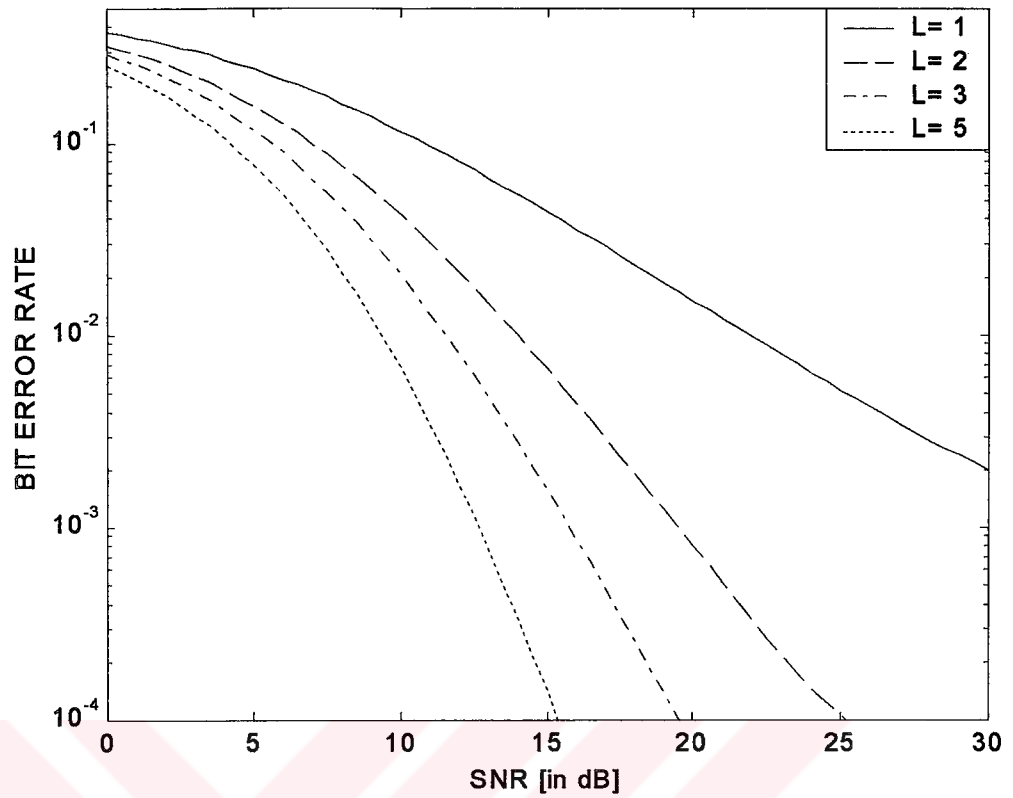


**Figure 4.2** Bit error rate for different values of selection combiner over a Rician-faded channel.

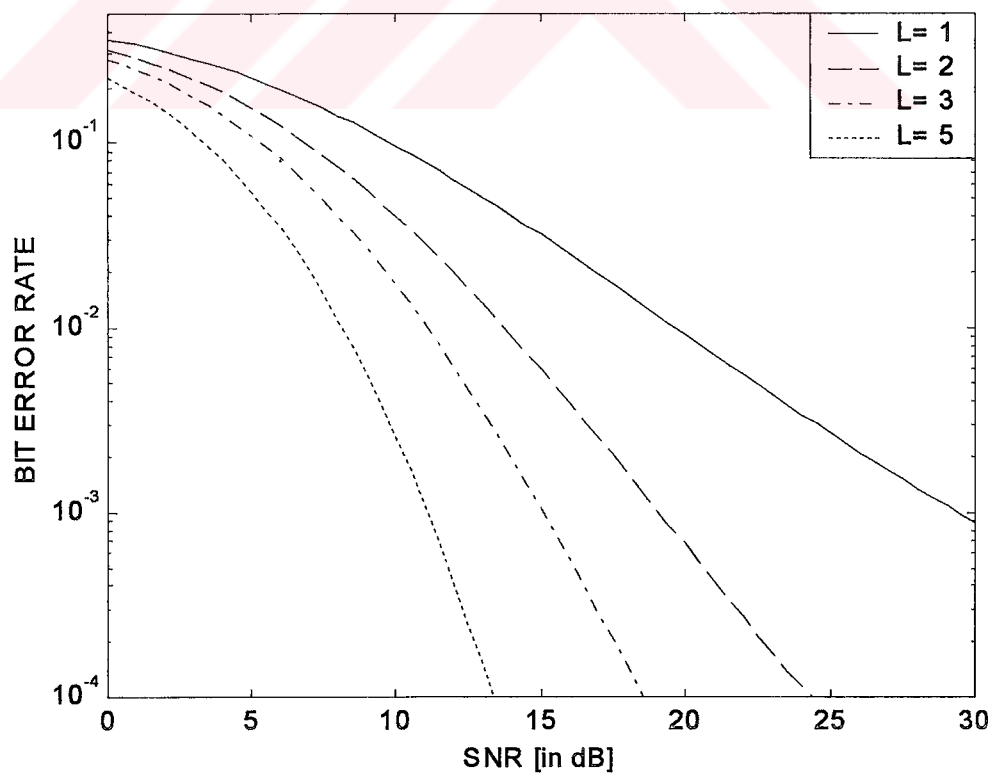


**Figure 4.3** Bit error rate for different values of maximal-ratio combiner over a Rician-faded channel.

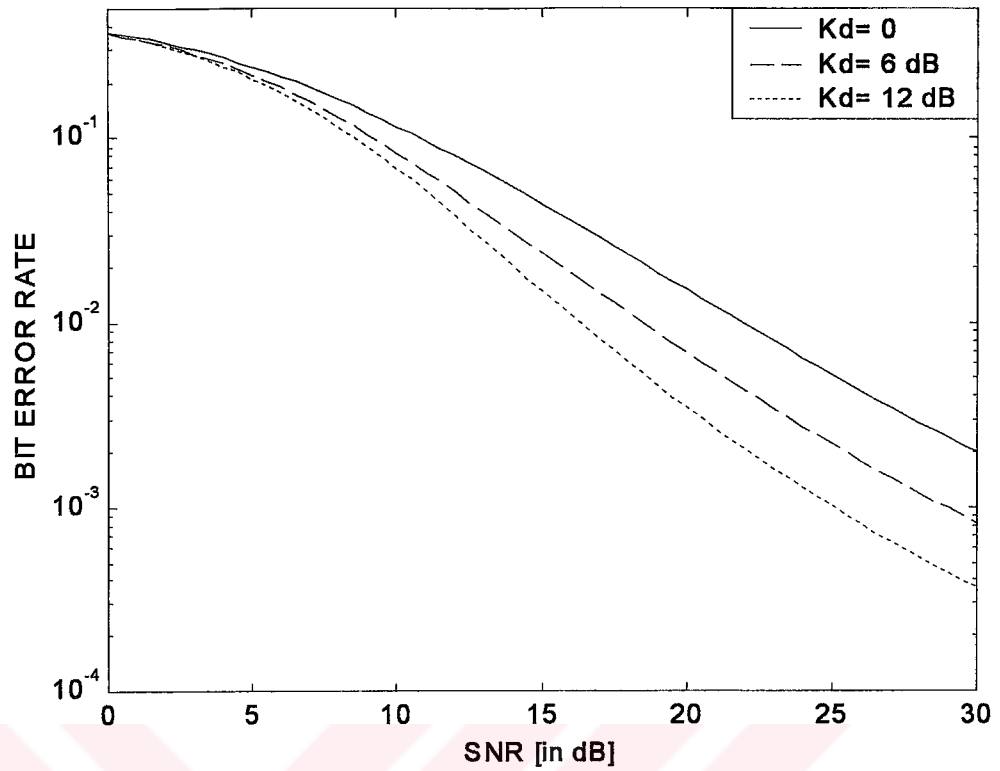


**Figure 4.4** Bit error rate for selection combining ( $L=1$ ) and several values of Rice-factor  $K_d$  over a Rician-faded channel.

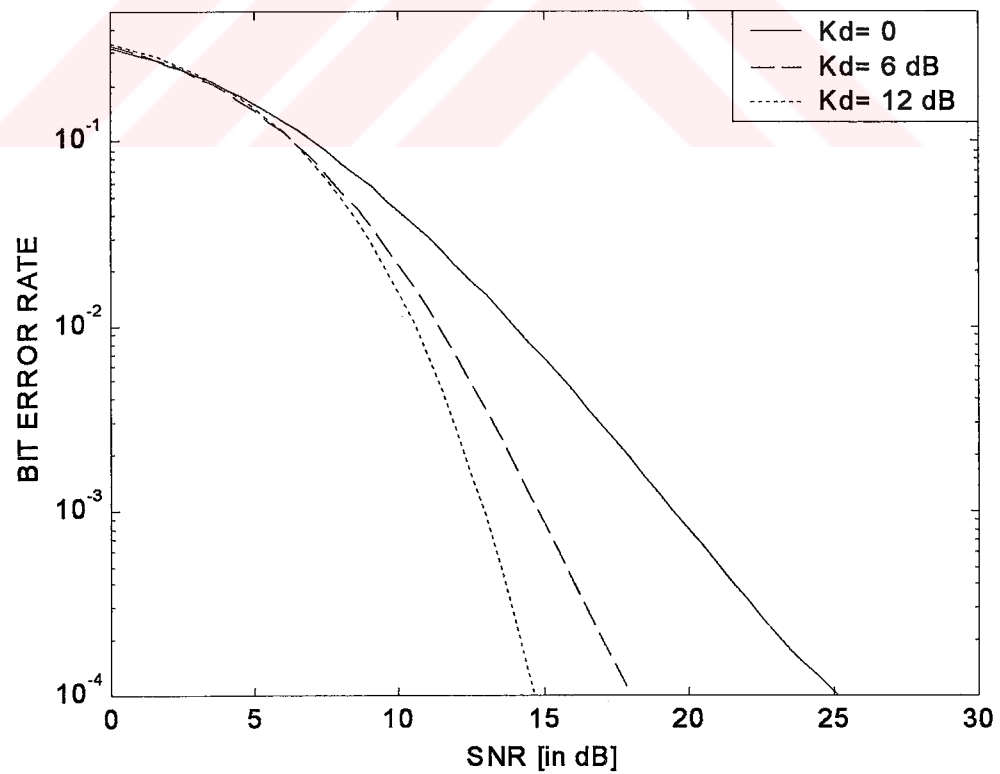


**Figure 4.5** Bit error rate for selection combining ( $L=2$ ) and several values of Rice-factor  $K_d$  over a Rician-faded channel.

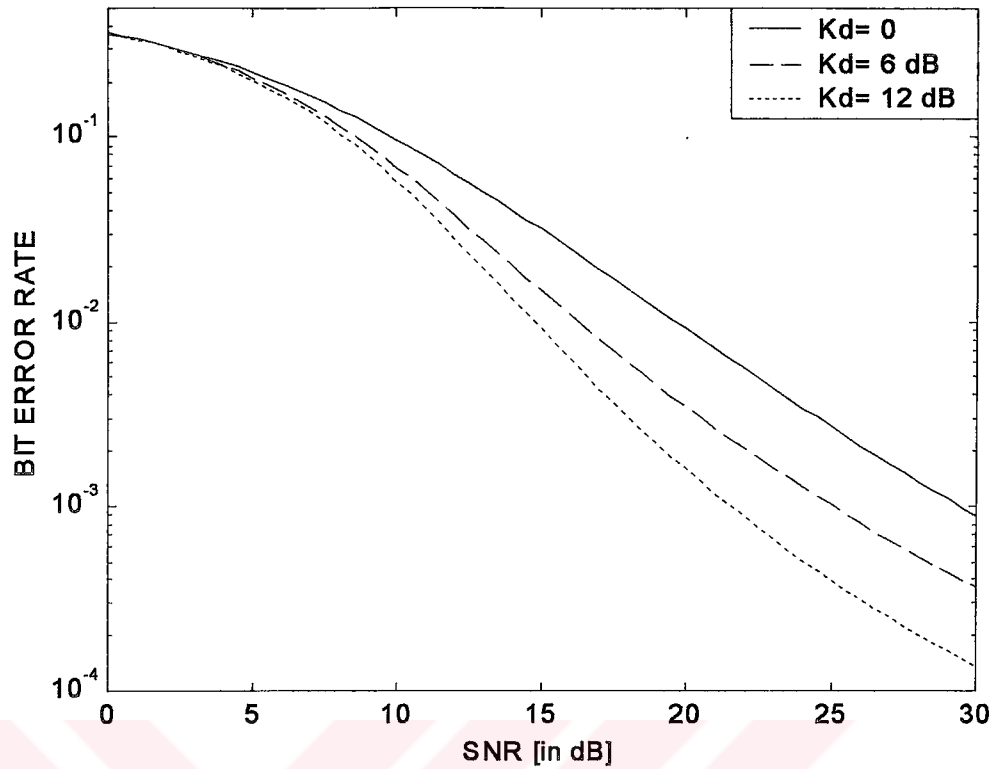


**Figure 4.6** Bit error rate for maximal-ratio combining ( $L=1$ ) and several values of Rice-factor  $K_d$  over a Rician-faded channel.

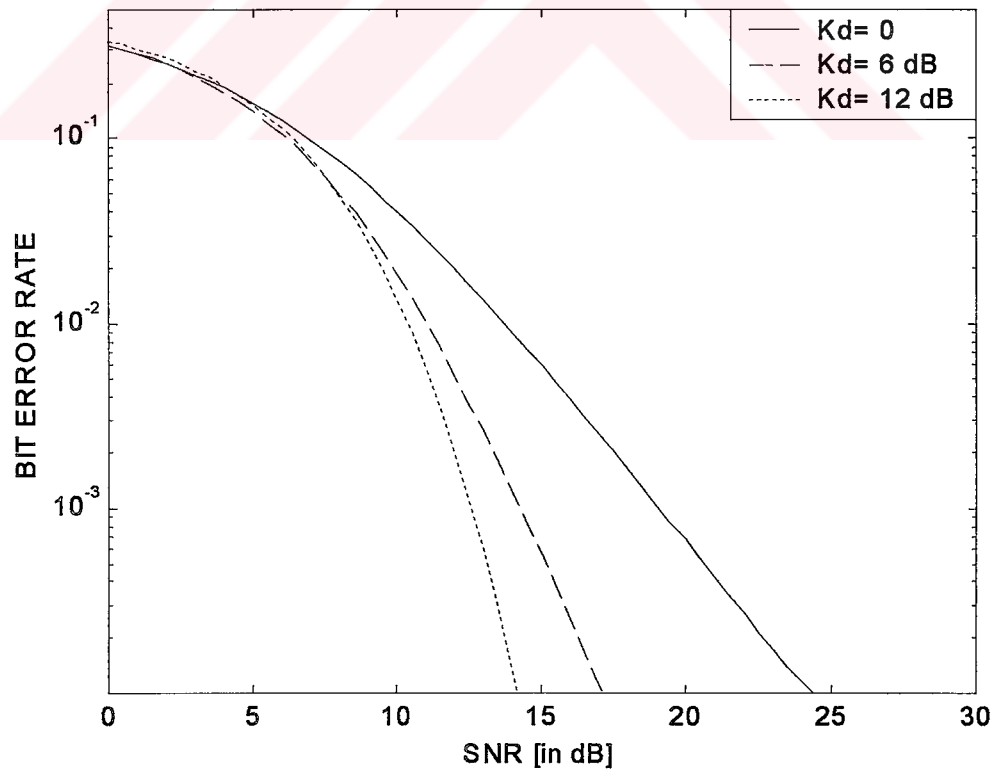


**Figure 4.7** Bit error rate for maximal-ratio combining ( $L=2$ ) and several values of Rice-factor  $K_d$  over a Rician-faded channel.

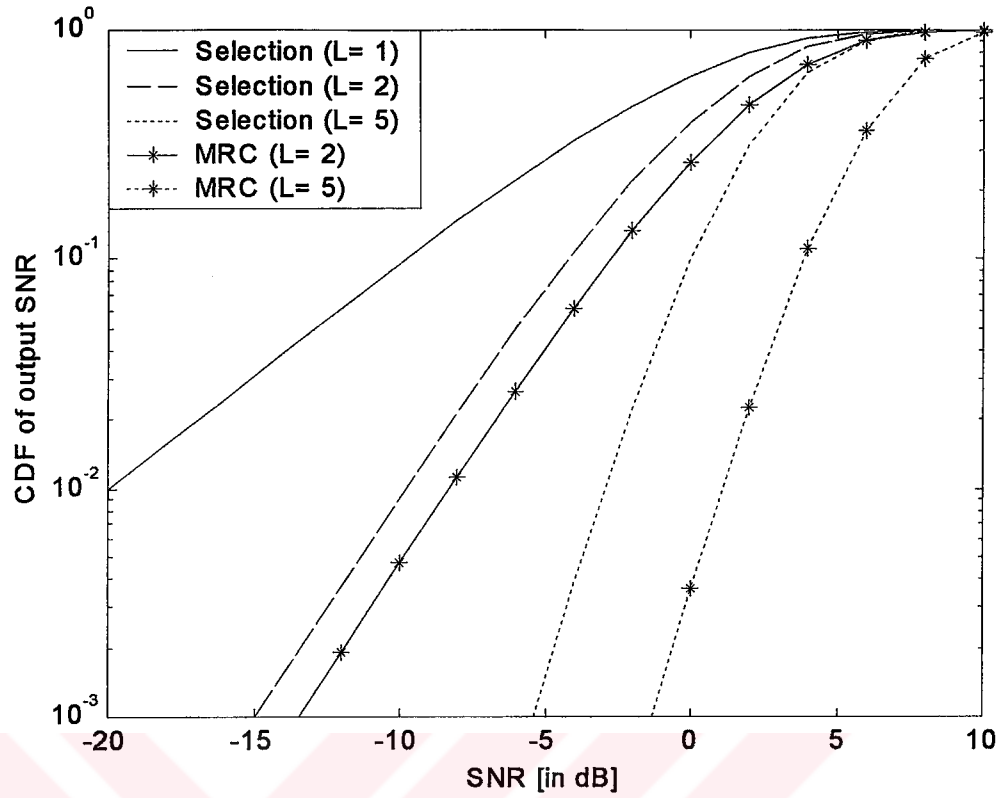


**Figure 4.8** Comparison of Selection combining and MRC techniques for several values of L.

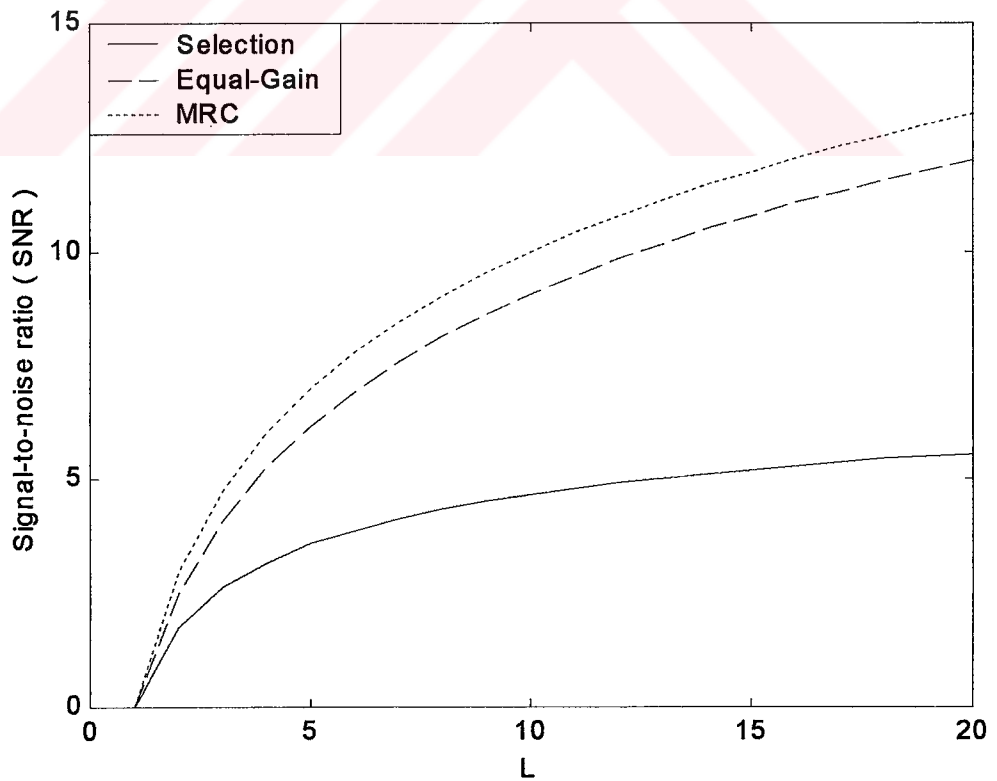


**Figure 4.9** Performance comparison improvement of various combining techniques for signal-to-noise ratio SNR and the number of diversity branches L.



## CHAPTER 5

### ADAPTIVE ANTENNA ARRAYS

An application of antenna arrays has been suggested in recent years for mobile communications systems to overcome the problem of limited channel bandwidth, thereby satisfying an ever growing demand for a large number of mobiles on communications channels. It has been shown by many studies that when an array is appropriately used in a mobile communications system, it helps in improving the system performance by increasing channel capacity and spectrum efficiency, extending range coverage. It also reduces multipath fading, co channel interferences and BER.

An array of antennas may be used in a variety of ways to improve the performance of a communications system. Perhaps most important is its capability to cancel co channel interferences. An array works on the premise that the desired signal and unwanted cochannel interferences arrive from different directions. The beam pattern of the array is adjusted to suit the requirements by combining signals from different antennas with appropriate weighting.

In a phased array receiving antenna, the signals received by the array elements are generally added at RF to form a receiving beam. In an adaptive array, an adaptive network controls the phase and amplitude of each elements output, that is, they use algorithms that iteratively adjust the weighting of the signals at the array elements. The signals are combined to maximize the signal-to-interference-plus-noise ratio (SINR) and to eliminate interfering signals in any direction other than the main beam.

In most cases, the elements of an array are identical. This is not necessary, but it is often convenient, simpler, and more practical. The individual elements of an array may be of any form (wires, apertures, etc.)

In an array of identical elements, there are five controls that can be used to shape the overall pattern of the antenna. These are:

1. The geometrical configuration of the overall array (linear, circular, rectangular, spherical, etc.).
2. The relative displacement between the elements.
3. The excitation amplitude of the individual elements.
4. The excitation phase of the individual elements.
5. The relative pattern of the individual elements.

The simplest and one of the most practical arrays is formed by placing the elements along a line as shown in Figure 5.1. In this study a uniformly spaced linear array is considered.

The adaptive array consists of a number of antenna elements coupled together via some form of amplitude control and phase shifting network to form a single output. The amplitude and phase control can be regarded as a set of complex weights as shown in Figure 5.2. The weights are controlled depending on the signal and the noise/interference environment as well as by the system requirements.

The signal at the output of each of the antenna elements is  $x_0(t), x_1(t), \dots, x_{\mu-1}(t)$ . The beam (assumed receiving) is formed by multiplying each output elements by corresponding complex weight and then summing the resultant signals. Both weights and output elements are complex quantities in that they are variable in phase and amplitude.

By suitable choice of complex conjugate phase shifts in the weights, a beam can be steered to the direction of the desired off-bore sight angle,  $\theta_d$ , which gives a coherent summation of the individual input and other than at  $\theta_i$ .

In cellular application, when used at the based stations, they are capable of providing automatic adjustment of the far field pattern to form nulls in the direction of interfering sources while, maintaining high gain in the direction of the desired user.

## 5.1 LINEAR ARRAY

The antenna elements can be arranged in various geometries: linear, circular and planar. In this thesis a uniformly spaced linear array (ULA) geometry is studied.

In Figure 5.1 a uniformly spaced linear array is depicted with  $\mu$  identical isotropic elements. Each element is weighted with a complex weight  $w_k$  with  $k = 0, 1, \dots, \mu - 1$  and the interelement spacing is denoted by  $d$ . If a plane wave impinges upon the array at an angle  $\theta$  with respect to the array normal, the wave front arrives at element  $k + 1$  sooner than at element  $k$ , since the differential distance along the two ray paths is  $d \sin \theta$ . By setting the phase of the signal at the origin arbitrarily to zero, the phase lead of the signal at element  $k$  relative to that at element 0 is  $nkd \sin \theta$ , where  $k = 2\pi / \lambda$  and  $\lambda$  is the wavelength of the signal. Adding all the element outputs together gives what is commonly referred to as array factor or pattern F:

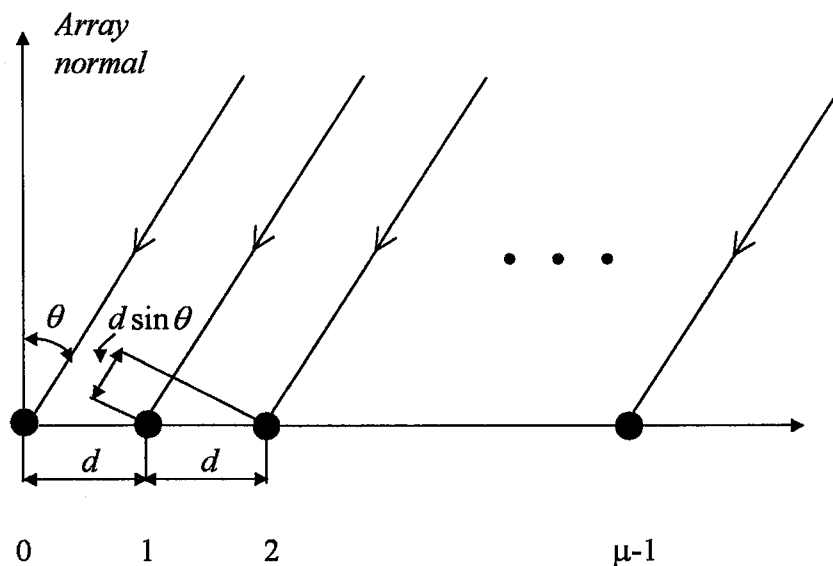


**Figure 5.1** A uniformly spaced linear array ( ULA )

$$F(\theta) = \sum_{n=0}^{\mu-1} w_n e^{jnk d \sin \theta} \quad (5.1)$$

which can be expressed in terms of vector inner product:

$$F(\theta) = w^T v \quad (5.2)$$

where  $w = [w_0 \ w_1 \ \dots \ w_{\mu-1}]^T$  (5.3)

is the weighting vector and

$$v = [1 \ e^{jkd \sin \theta} \ \dots \ e^{j(\mu-1)kd \sin \theta}]^T \quad (5.4)$$

is the steering vector that contains the information on the angle of arrival (AOA) of the signal.

## 5.2 OPERATION OF ADAPTIVE ANTENNA ARRAYS

The adaptive array consists of a number of antenna elements coupled together via some form of amplitude control and phase shifting network to form a single output. The amplitude and phase control can be regarded as a set of complex weights, as illustrated in Figure 5.2. If the effects of receiver noise and mutual coupling are ignored, the operation of an  $\mu$  element uniformly spaced linear array can be explained as follows. Consider a wave front generated by a narrow-band source of wavelength  $\lambda$  arriving at an  $\mu$  element array from a direction  $\theta_i$  off the array boresight. Now taking the first element in the array as the phase reference and letting  $d$  equal the array spacing, the relative phase shift of the received signal at the  $m^{\text{th}}$  element can be expressed as

$$\phi_{mi} = \frac{2\pi d m}{\lambda} \sin \theta_i \quad (5.5)$$

Assuming constant envelope modulation of the source at  $\theta_i$ , the signal at the output of each of the antenna elements can be expressed as

$$x_{mi}(t) = e^{j(\omega t + \phi_{mi})} \quad (5.6)$$

and the total array output in the direction  $\theta_i$  as

$$y_i(t) = \sum_{m=0}^{\mu-1} w_m e^{j(\omega t + \phi_{mi})} \quad (5.7)$$

where  $w_m$  represents the value of the complex weight applied to the output of the  $m^{\text{th}}$  element. Thus by suitable choice of weights, the array will accept a wanted signal from direction  $\theta_i$  and steer nulls toward interference sources located at  $\theta_j$ . Likewise, the weighting network can be optimized to steer beams in a specific direction, or directions.

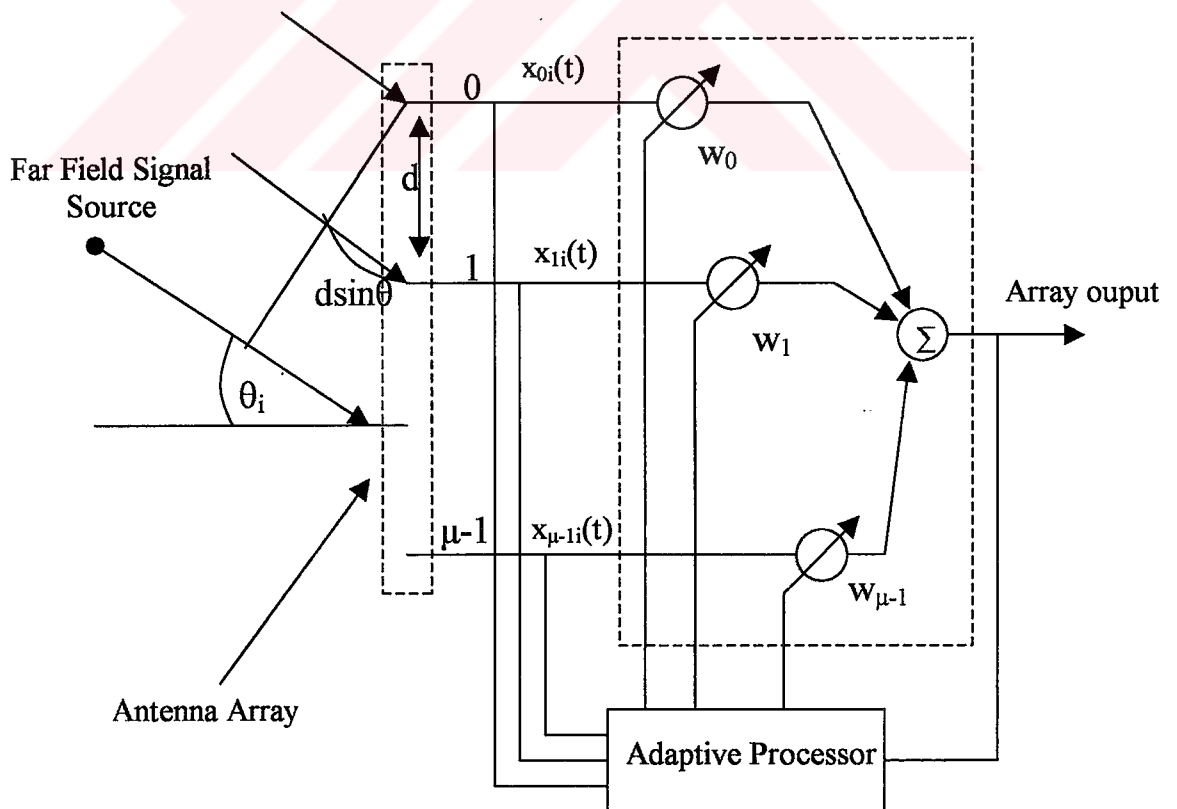


Figure 5.2 Adaptive antenna array

### 5.3 SIMULATION RESULTS

In this section, some simulation results will be reported which illustrate the array pattern configurations of a uniformly spaced linear array (ULA) for several values of antenna element  $\mu$  and interelement spacing  $d$ . It is assumed that the signal is coming at an angle of  $\theta_1$ .

In Figure 5.3, the variations of the magnitude of the array pattern for several values of  $\mu$  with a common element spacing of  $d = \lambda/2$  are illustrated. The antenna elements are typically sited  $\lambda/2$  apart, where  $\lambda$  is the wavelength of the received signal. Spacing of greater than  $\lambda/2$  improves the spatial resolution of the array, however, the formation of grating lobes (secondary maxima) can also result. These are generally regarded as undesirable. On the target direction of interest,  $\theta_1$ , a particular beam is identified as the *main beam* and the remainder are viewed as auxiliary beams. Each of the auxiliary beams has a *null in the look direction of the main beam*. With  $\mu$  antennas, the system is capable of placing up to  $\mu - 1$  nulls along the (unknown) directions of independent interferences. As the number of antenna elements increases, the beam width of the main beam decreases so the antenna array focuses towards the target direction of interest better.

In Figure 5.4, array patterns in polar coordinates for  $\mu=2$  and  $\mu=4$  with a common element spacing  $d = \lambda/2$  are illustrated.

In Figure 5.5, array patterns in polar coordinates for  $\mu=8$  and  $\mu=16$  with a common element spacing  $d = \lambda/2$  are illustrated.

In Figure 5.6, array patterns in polar coordinates for  $\mu=32$  and  $\mu=64$  with a common element spacing  $d = \lambda/2$  are illustrated.

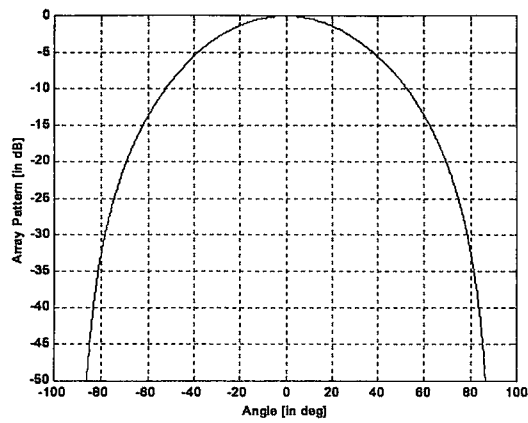
In Figure 5.7, the variations of the magnitude of the array pattern for different element spacing with an equal sized aperture of length  $10\lambda$  are illustrated. There is no

so much difference between  $d = \lambda/4$  and  $d = \lambda/2$ . There is only one main beam towards the target direction of interest in two cases. But, when the interelement spacing  $d$  is greater than  $\lambda/2$ , there is more than one main beam, which is called “the grating lobe” or secondary maximal. It can be easily seen when  $d = \lambda$  and  $d = 2\lambda$ . Of course, this is an undesired case, because the antenna array pattern is not only steered towards the target direction of interest, but it has also grating lobes towards the other directions such as  $-30$  and  $30$ . This means, the system wastes power towards the undesired directions.

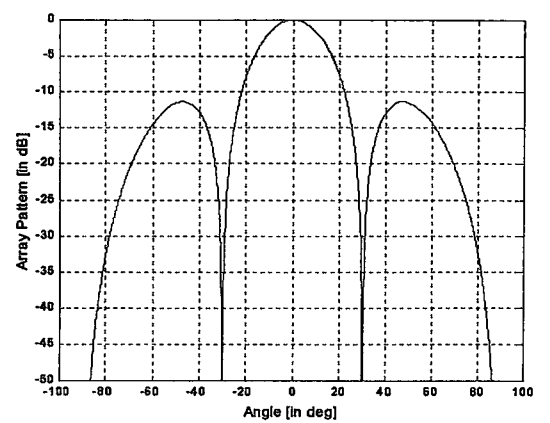
In Figure 5.8, array patterns in polar coordinates for  $d = \lambda/8$  and  $d = \lambda/4$  with an equal sized aperture of length  $10\lambda$  are illustrated.

In Figure 5.9, array patterns in polar coordinates for  $d = \lambda/2$  and  $d = \lambda$  with an equal sized aperture of length  $10\lambda$  are illustrated.

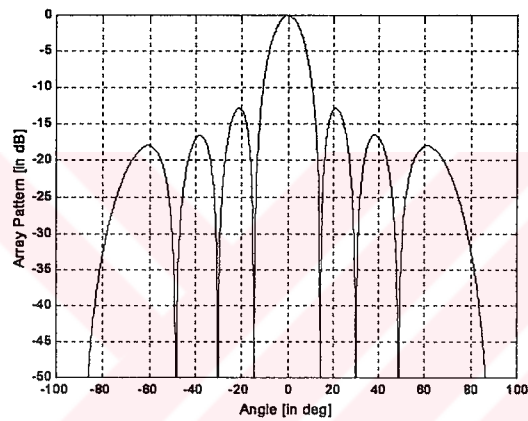
In Figure 5.10, array patterns in polar coordinates for  $d = 2\lambda$  and  $d = 4\lambda$  with an equal sized aperture of length  $10\lambda$  are illustrated.



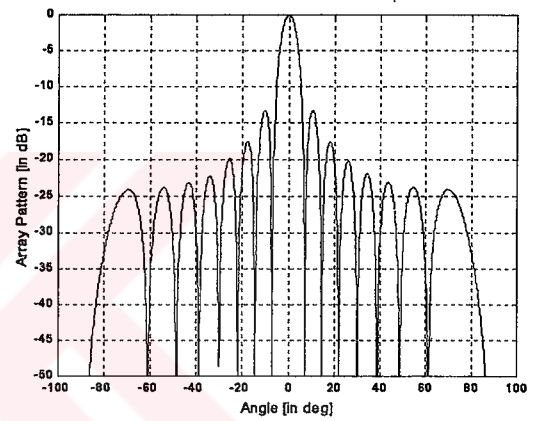
(a)  $\mu=2$



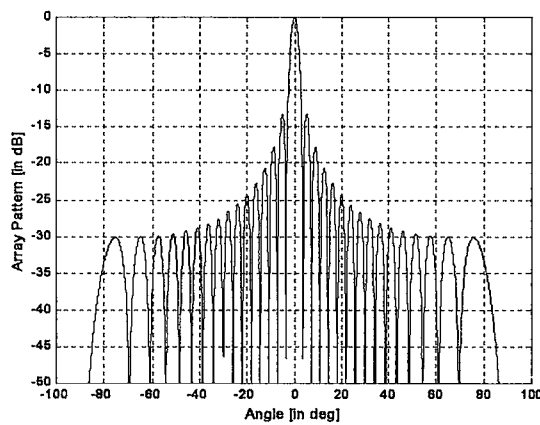
(b)  $\mu=4$



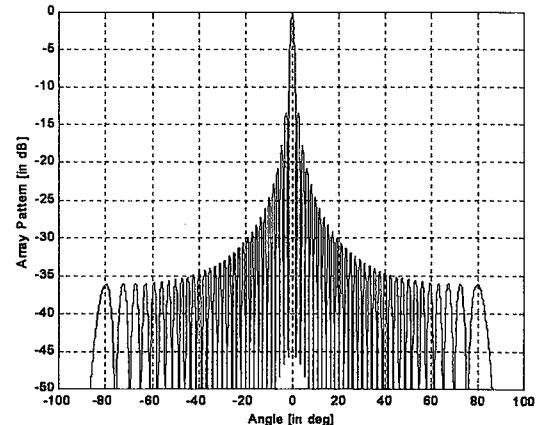
(c)  $\mu=8$



(d)  $\mu=16$



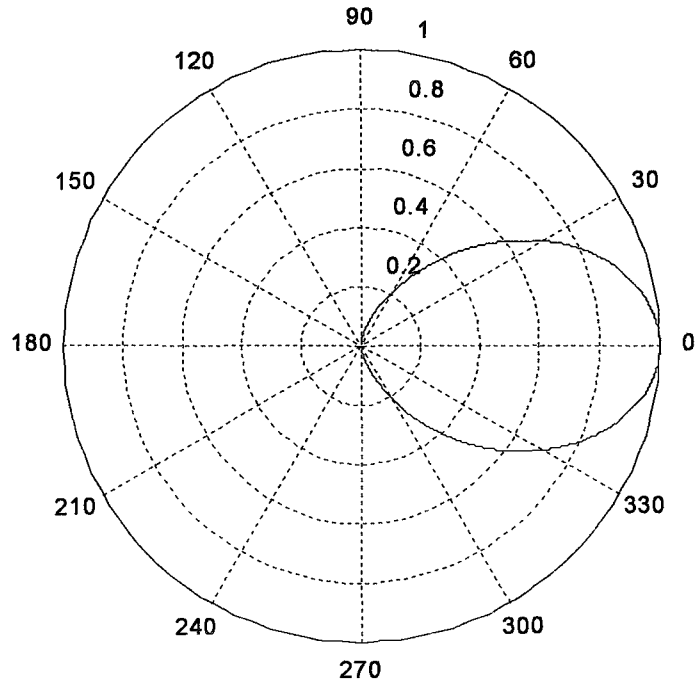
(e)  $\mu=32$



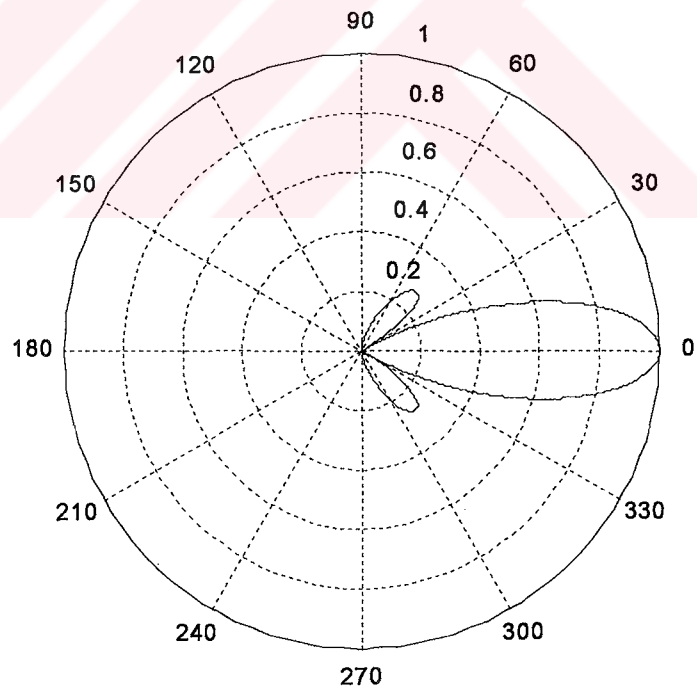
(f)  $\mu=64$

**Figure 5.3.** Array patterns in rectangular coordinates for several values of  $\mu$  with a common element spacing of  $d = \lambda/2$ .



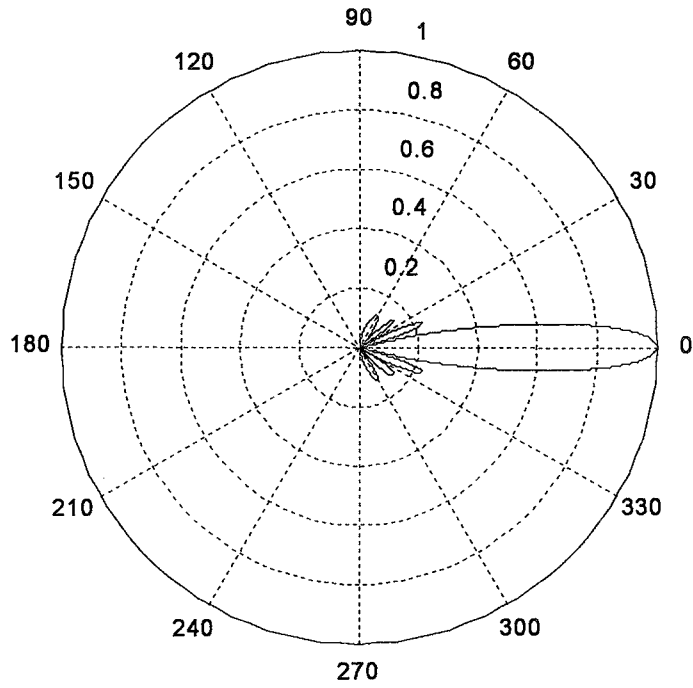


(a)  $\mu=2$

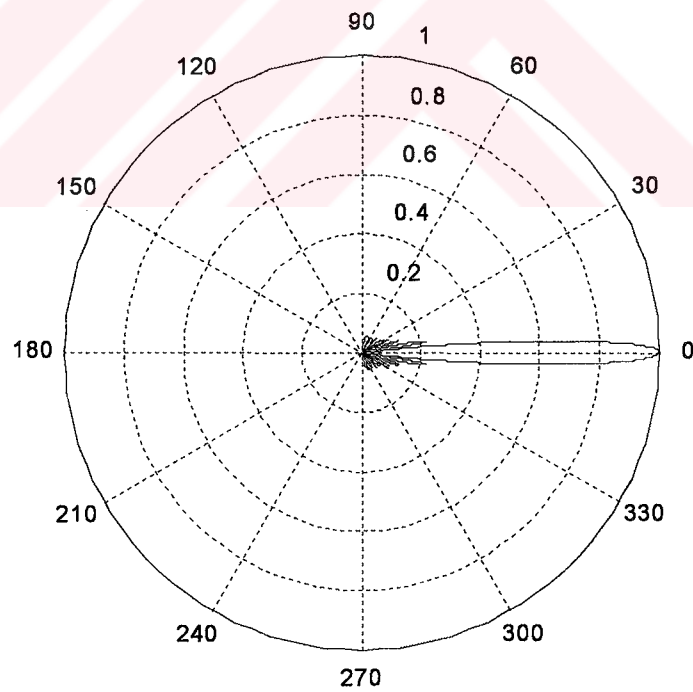


(b)  $\mu=4$

**Figure 5.4** Array patterns in polar coordinates for  $\mu=2$  and  $\mu=4$  with a common element spacing  $d= \lambda/2$ .

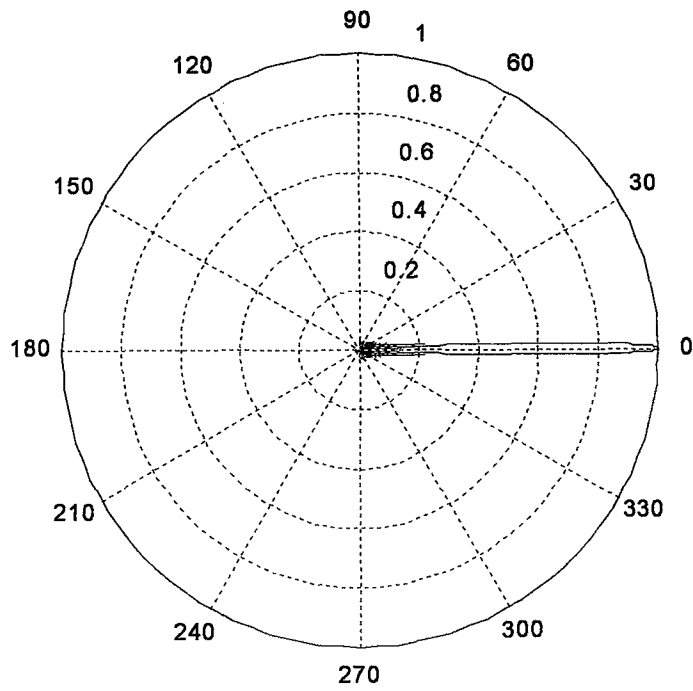


(c)  $\mu=8$

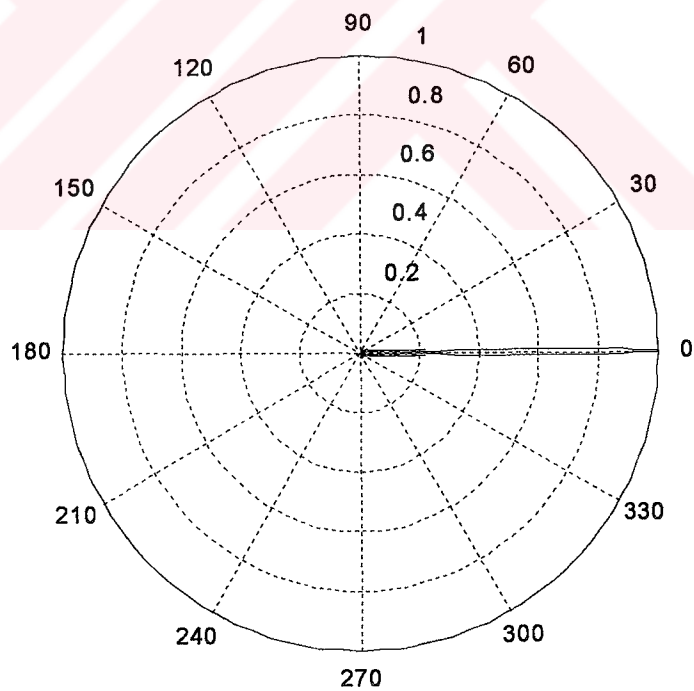


(d)  $\mu=16$

**Figure 5.5** Array patterns in polar coordinates for  $\mu=8$  and  $\mu=16$  with a common element spacing  $d= \lambda/2$ .

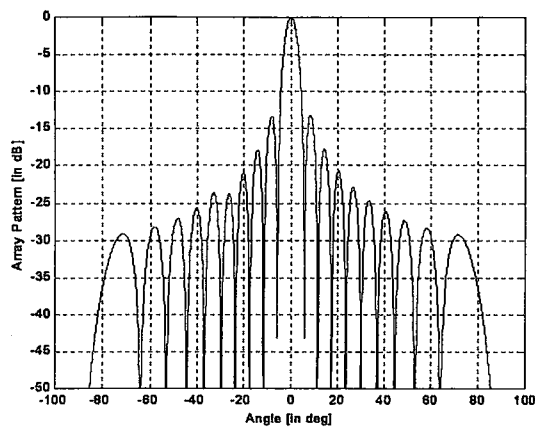


(e)  $\mu=32$

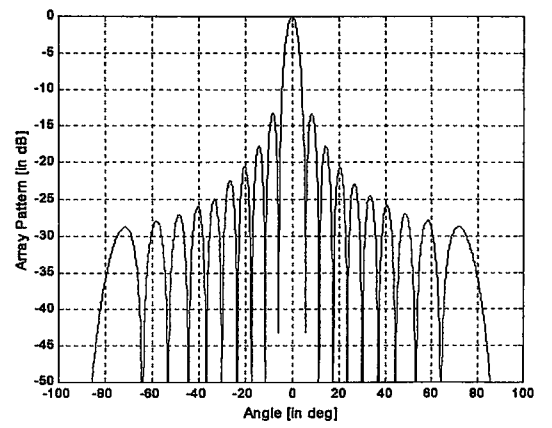


(f)  $\mu=64$

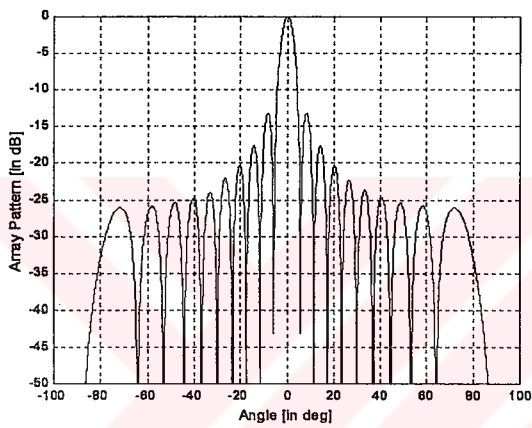
**Figure 5.6** Array patterns in polar coordinates for  $\mu=32$  and  $\mu=64$  with a common element spacing  $d= \lambda/2$ .



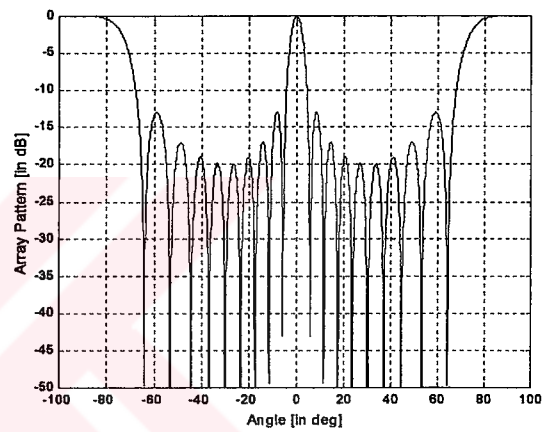
(a)  $d = \lambda/8$



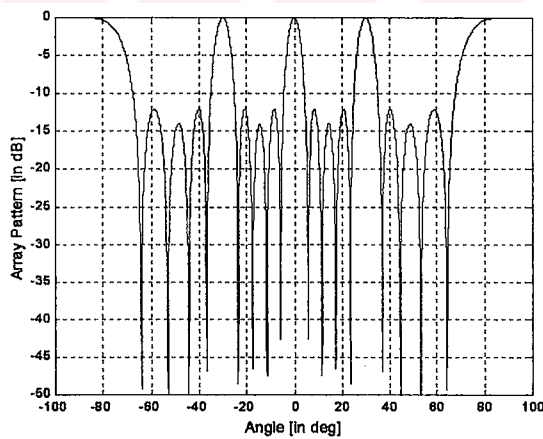
(b)  $d = \lambda/4$



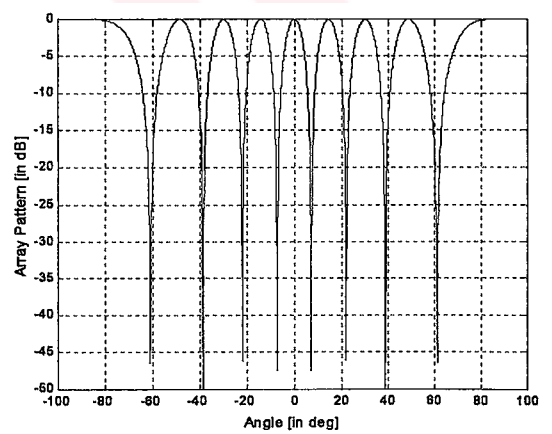
(c)  $d = \lambda/2$



(d)  $d = \lambda$

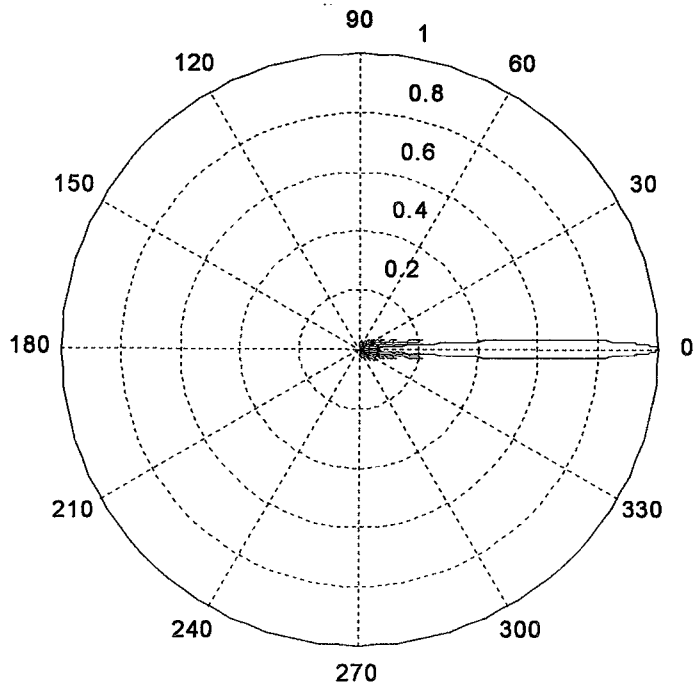


(e)  $d = 2\lambda$

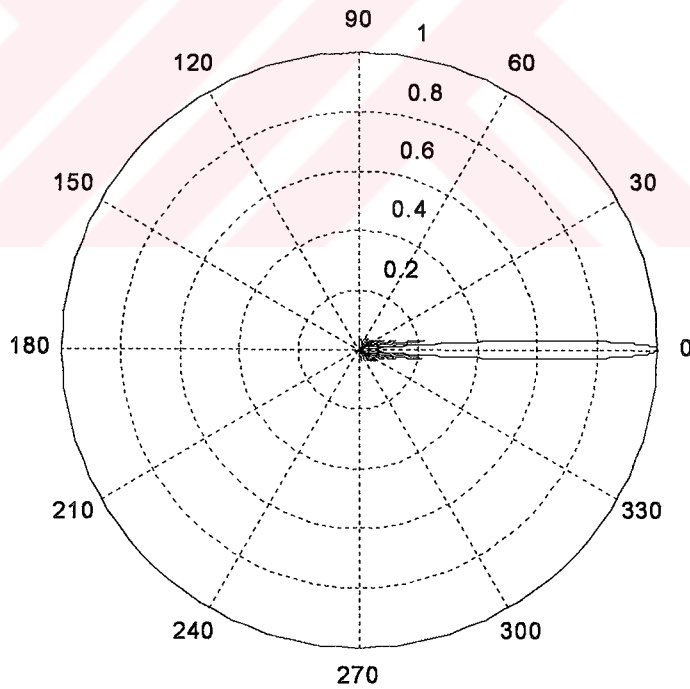


(f)  $d = 4\lambda$

**Figure 5.7** Array patterns in rectangular coordinates for different element spacings with an equal sized aperture of length  $10\lambda$ .

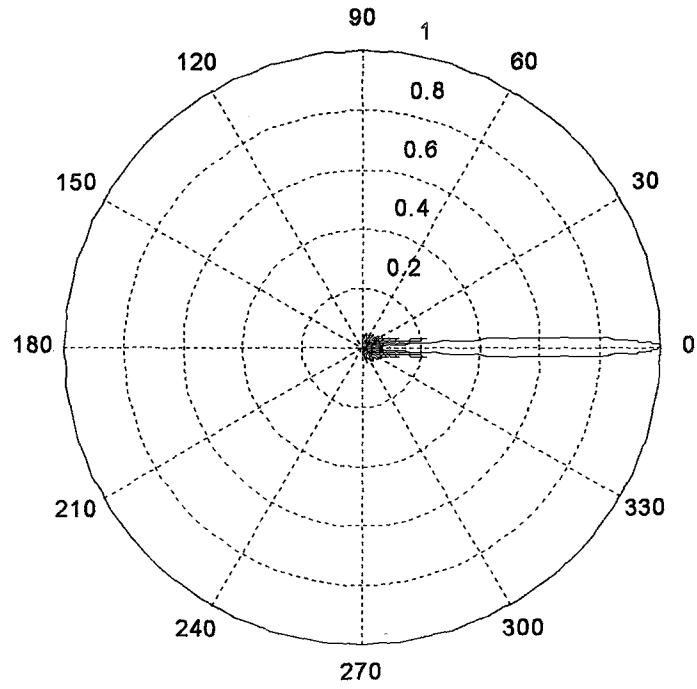


(a)  $d = \lambda/8$

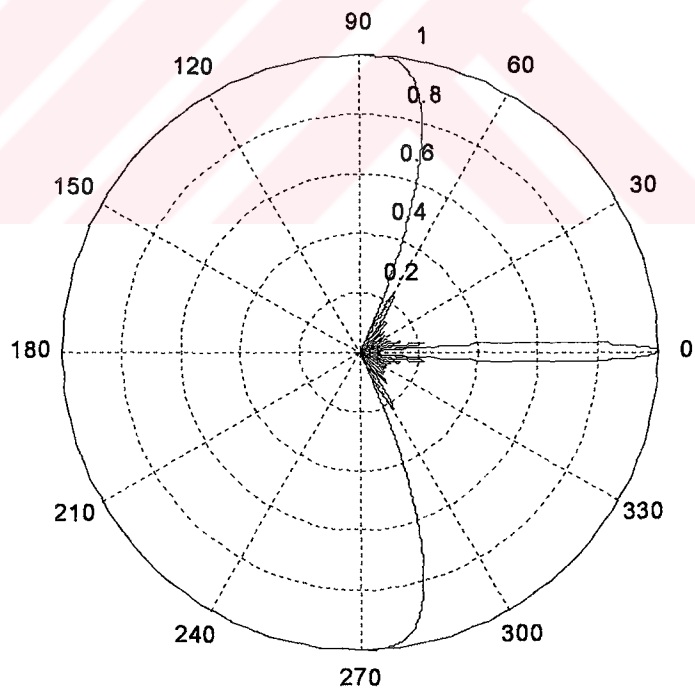


(b)  $d = \lambda/4$

**Figure 5.8** Array patterns in polar coordinates for  $d = \lambda/8$  and  $d = \lambda/4$  with an equal sized aperture of length  $10\lambda$ .

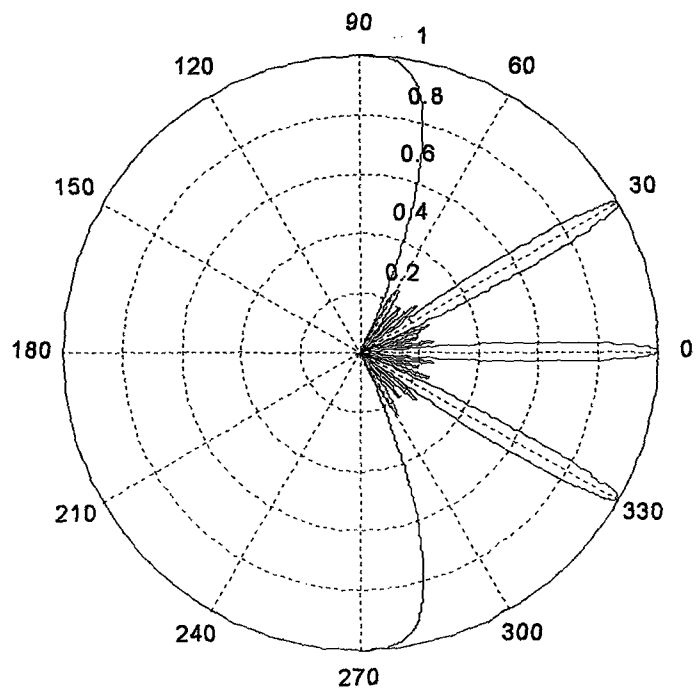


(c)  $d = \lambda/2$

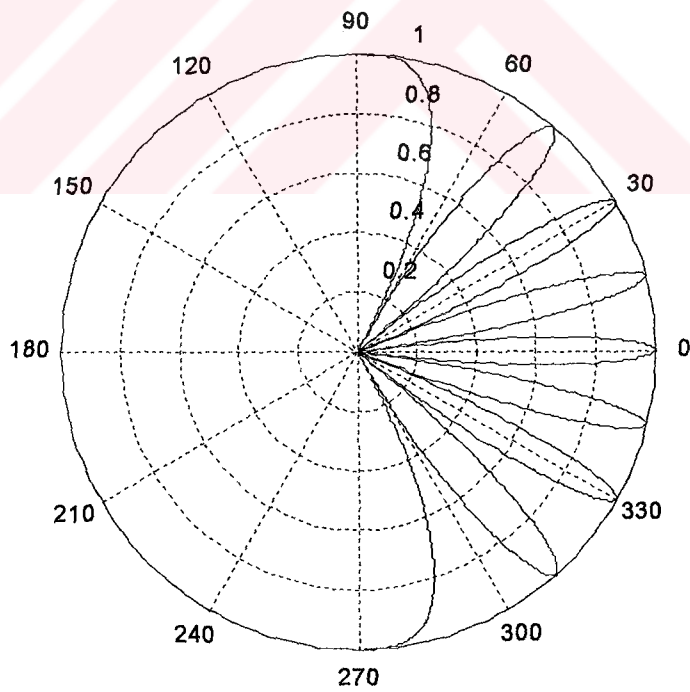


(d)  $d = \lambda$

**Figure 5.9** Array patterns in polar coordinates for  $d = \lambda/2$  and  $d = \lambda$  with an equal sized aperture of length  $10\lambda$ .



(e)  $d = 2\lambda$



(f)  $d = 4\lambda$

**Figure 5.10** Array patterns in polar coordinates for  $d = 2\lambda$  and  $d = 4\lambda$  with an equal sized aperture of length  $10\lambda$ .

## CHAPTER 6

### ADAPTIVE BEAMFORMING

The term beamforming derives from the fact that early spatial filters were designed to form pencil beams in order to receive a signal radiating from a specific location and attenuate signals from other locations. Forming beams seems to indicate radiation of energy. However, beamforming is applicable to either radiation or reception of energy.

System designed to receive spatially propagation signals often encounter the presence of interference signals. If the desired signal and interferers occupy the same temporal frequency band, then temporal filtering can not be used to separate signal from interference. However, the desired and interfering signals usually originate from different spatial locations. This spatial separation can be exploited to separate signal from interference using a spatial filter at the receiver. Implementing a temporal filter requires processing of data collected over a temporal aperture. Similarly, implementing a spatial filter requires processing of data collected over a spatial aperture.

When the spatial sampling is discrete, the processor that performs the spatial filtering is termed a beamformer. A beamformer linearly combines the spatially sampled time series from each sensor to obtain a scalar output time series. Beamformers, can be classified as either data independent or statistically optimum, depending on how the weights are chosen. The weights in a data independent beamformer do not depend on the array data and are chosen to present a specified response for all signal/interference scenarios. The weights in a statistically optimum beamformer are chosen based on the statistics of the array data to optimize the array response. In general, the statistically optimum beamformer places nulls in the directions of interfering sources in a attempt to maximize the signal-to-noise ratio at the beamformer output.



Data independent beamformer design techniques are often used in statistically optimum beamforming. The statistics of the array data are not usually known and may change over time so adaptive algorithms are typically employed to determine the weights. The adaptive algorithm is designed so the beamformer response converges to a statistically optimum solution. Partially adaptive beamformers reduce the adaptive algorithm computational load at the expense of a loss in statistical optimality.

Adaptive beamformers, also termed adaptive antenna arrays, on the other hand, are able to listen to a particular subscriber and deliver energy to that subscriber more efficiently. They can place nulls in the direction of interferers via adaptive updating of weights linked to each antenna element. They thus cancel out most of the cochannel interference resulting in better quality of reception. These systems usually consist of a set of antenna elements that can change their antenna radiation or reception pattern dynamically to adjust to variations in channel noise and interference, in order to improve the output signal-to-noise ratio (SNR) of a desired signal.

The basic objective of an adaptive beamformer is to adjust the complex weights at the output of each array element so as to produce a pattern that optimizes the reception of a target signal along a direction of interest in the presence of noise and cochannel interference, in some statistical sense.

## **6.1 THE SPATIAL FILTERING PROBLEM**

### **6.1.1 Statement**

Consider an antenna array that receives various signals from several directions in space. The spatial filtering problem is to *optimize* the antenna pattern such that *maximum possible gain* is placed on the direction on the desired signal and *nulls* are placed on the directions of the interferers.

### 6.1.2 Problem Setup

Let  $s_d(t)$  denote the desired communications signal arriving at the array at an angle  $\theta_d$  and  $s_i(t)$  denote the  $N$  interfering signals arriving at the array at angle of incidences  $\theta_i$  respectively. It is assumed here that the adaptive processor has no a priori knowledge of the directions of arrivals (DOA's) of both the signal and the interferers. The signal received by the antenna array is given by,

$$x(t) = s_d(t)v(\theta_d) + s_n + \sum_{i=1}^N s_i(t)v(\theta_i) \quad (6.1)$$

where,

$x(t)$  - The received signal (output of antenna array) vector of  $\mu \times 1$ .

$v(\theta_d)$  - The steering vector for the desired signal of  $\mu \times 1$ .

$v(\theta_i)$  - The steering vector for the  $i^{th}$  interfering signal of  $\mu \times 1$ .

$s_n$  - AWGN vector of  $\mu \times 1$ .

The generalized spatial filtering problem is to estimate the desired signal  $s_d(t)$  from the received signal  $x(t)$  such that the some measure of error between the estimated signal and the original signal  $s_d(t)$  is minimized. The mean squared error (MSE) criterion is normally used for optimization. In this case, the filtering problem can be setup as a classical Wiener Filtering problem for which the solution can be iteratively reached using the adaptive algorithms.

### 6.2 FUNDAMENTALS OF OPERATION

The adaptive array consists of a number of antenna elements, not necessarily identical, coupled together via some form of amplitude control and phase shifting network to form a single output. The amplitude and phase control can be regarded as a set of complex weights, as given in Figure 5.2.

The adaptive array used in this thesis is a Uniform Linear Array (ULA) of  $\mu$  elements. Each of the elements in the ULA is scaled by their corresponding weights and are summed to form the output signal. The weights are in turn controlled by an adaptive algorithm that operates on the received signal and the desired signal. Basically, the objective is to optimize the adaptive antenna array response with respect to prescribed criteria, so that the output  $y(t)$  contains minimal contribution from noise and interference. Minimum Mean Square error criteria will be discussed in section 6.3

The output of the adaptive antenna array is given by,

$$y(t) = w^H x(t) \quad (6.2)$$

where  $w$  represents the  $\mu$ - element weight vector and  $x$  represents the input signal vector received by the antenna array given in (6.1).

$$x(t) = \begin{bmatrix} x_0(t) \\ x_1(t) \\ \cdot \\ \cdot \\ x_{\mu-1}(t) \end{bmatrix} \quad (6.3)$$

The reference signal  $d(t)$  generated at the receiver is usually assumed to have similar statistical properties as the transmitted signal  $s_d(t)$ . Various methods are described in literature for generating this reference signal  $d(t)$ . The error signal  $e(t)$  is given by,

$$e(t) = d(t) - y(t) \quad (6.4)$$

### 6.3 MINIMUM MEAN - SQUARE ERROR (MMSE) CRITERIA

The Wiener-Hopf solution for the spatial filtering problem will be derived in this section [13].

Let us consider a uniformly spaced linear array, as shown in Figure 5.1, which operates in a signal environment where there is a desired communication signal  $s_d(t)$ , as well as  $L$  interfering signals  $s_i(t)$ . If the desired signal  $s_d(t)$  is known, one may choose to minimize the error between the beamformer output  $y(t)$  and the desired signal. Of course, knowledge of the desired signal eliminates the need for beamforming. However, for many applications, characteristics of the desired signal may be known with sufficient detail to generate a signal  $d(t)$  that closely represents it, or at least correlates with the desired signal to a certain extent. This signal is called a reference signal [14]. The weights are chosen to minimize the mean-square error (MSE) between the beamformer output and the reference signal:

$$e^2(t) = [d(t) - w^H x(t)]^2 \quad (6.5)$$

Taking the expected values of both sides of (6.5) and carrying out some basic algebraic manipulation, we have

$$E\{e^2(t)\} = E\{d^2(t)\} - 2w^H r + w^H R w \quad (6.6)$$

where

$R = E\{x(t)x^H(t)\}$  is the auto-correlation or covariance matrix of the received

signal, and

$r = E\{d(t)x(t)\}$  is the cross-correlation vector between the desired signal and the received signal.

The minimum MSE is obtained by setting the *gradient* vector of the above equation (6.6) with respect to  $w$  equal to zero:

$$\nabla_w (E\{e^2(t)\}) = -2r + 2Rw = 0 \quad (6.7)$$

It follows that the solution is

$$w_{opt} = R^{-1}r \quad (6.8)$$

which is referred to as the Wiener-Hopf equation or the optimum Wiener solution. These optimum weights can be calculated by a number of adaptive algorithms. These algorithms are discussed in Chapter 7

## CHAPTER 7

### ADAPTIVE ALGORITHMS

The choice of adaptive algorithms for deriving the adaptive weights is highly important in that it determines both the speed of convergence and hardware complexity required to implement the algorithm. In this chapter, we will discuss a number of common adaptive techniques. It should be pointed out that the criterion in the preceding chapter is described in continuous time. Obviously, they are also applicable to discrete-time signals. In this chapter, since we are dealing with digital adaptive beamforming algorithms, we will emphasize the digital signal processing aspects by expressing the algorithms in terms of discrete time.

#### 7.1 LEAST - MEAN - SQUARE ALGORITHM

The most common adaptive algorithm for continuous adaptation is the least-mean-square (LMS) algorithm. It has been studied and is well understood [2]. It is based on the steepest-descent method, a well-known optimization method [15], that recursively computes and updates the weight vector  $w$ . It is intuitively reasonable that successive corrections to the weight vector in the direction of the negative of the gradient vector should eventually lead to the MSE, at which point the weight vector assumes its optimum value. According to the method of steepest descent, the updated value of the weight vector at time  $n + 1$  is computed by using the simple recursive relation,

$$w(n+1) = w(n) + \frac{1}{2}\alpha[-\nabla(E\{e^2(n)\})] \quad (7.1)$$

It follows from (6.7) that

$$w(n+1) = w(n) + \alpha[r - Rw(n)] \quad (7.2)$$

In reality, an exact measurement of the gradient vector is not possible, since this would require a prior knowledge of both  $R$  and  $r$ . The most obvious strategy is to use their instantaneous estimates, which are defined, respectively, as

$$\hat{R} = x(n)x^H(n) \quad (7.3)$$

And

$$\hat{r} = d(n)x(n) \quad (7.4)$$

The weights can then be updated as

$$w(n+1) = w(n) + \alpha x(n)[d(n) - x^H(n)w(n)] \quad (7.5)$$

Using the expressions for the error (6.5) and the output (6.2) in the above equation (7.5), we get the LMS algorithm as:

$$\text{Output, } y(n) = w^H x(n) \quad (7.6)$$

$$\text{Error, } e(n) = d(n) - y(n) \quad (7.7)$$

$$\text{Weight, } w(n+1) = w(n) + \alpha x(n)e^*(n) \quad (7.8)$$

The step size parameter  $\alpha$  controls convergence characteristics of the random vector sequence  $w(n)$ . Starting with an arbitrary initial weight vector, the LMS algorithm will converge and stay stable in the mean square if and only if the step-size parameter  $\alpha$  satisfies the condition:

$$0 < \alpha < \frac{2}{\lambda_{\max}} \quad (7.9)$$

where  $\lambda_{\max}$  is the largest eigenvalue of the Covariance Matrix,  $R$ . The primary virtue of the LMS algorithm is its simplicity. Its performance is acceptable in many applications. However, its convergence characteristics depend on the eigenstructure of

$\hat{R}$ . When the eigenvalues are widely spread, convergence can be slow and other adaptive algorithms with better convergence rates should be considered.

## 7.2 RECURSIVE LEAST - SQUARES ALGORITHM

We can estimate  $R$  and  $r$  using the weighted sum:

$$\hat{R}(n) = \sum_{i=1}^n \gamma^{n-i} x(i)x^H(i) \quad (7.10)$$

and

$$\hat{r}(n) = \sum_{i=1}^n \gamma^{n-i} d(i)x(i) \quad (7.11)$$

The weighting factor,  $0 < \gamma \leq 1$ , is intended to ensure that data in the distant past are “forgotten” in order to allow the processor to follow the statistical variations of the observable data. Factoring out the terms corresponding to  $i = n$  in both (7.10) and (7.11), we have the following recursion for updating both  $\hat{R}(n)$  and  $\hat{r}(n)$  :

$$\hat{R}(n) = \gamma \hat{R}(n-1) + x(n)x^H(n) \quad (7.12)$$

and

$$\hat{r}(n) = \gamma \hat{r}(n-1) + d(n)x(n) \quad (7.13)$$

The inverse of the covariance matrix is given by the following recursive equation,

$$\hat{R}^{-1}(n) = \gamma^{-1}[\hat{R}^{-1}(n-1) - k(n)x(n)\hat{R}^{-1}(n-1)] \quad (7.14)$$

where the gain vector  $k(n)$  is given by [2] :

$$k(n) = \frac{\gamma^{-1}\hat{R}^{-1}(n-1)x(n)}{1 + \gamma^{-1}x^H(n)\hat{R}^{-1}(n-1)x(n)} \quad (7.15)$$



To develop the recursive equation for updating the least squares estimate  $w(n)$ , we use (6.8) to express  $w(n)$  as follows:

$$\begin{aligned} w(n) &= \hat{R}^{-1}(n)\hat{r}(n) \\ &= \gamma^{-1}[\hat{R}^{-1}(n-1) - k(n)x(n)\hat{R}^{-1}(n)] \times [\gamma r(n-1) + d(n)x(n)] \end{aligned} \quad (7.16)$$

Rearranging the above equation, the desired recursive equation for updating the weight vector is given by,

$$\begin{aligned} w(n) &= w(n-1) + k(n)[d(n) - w^H(n-1)x(n)] \\ &= w(n-1) + k(n)e^*(n) \end{aligned} \quad (7.17)$$

where  $e(n)$  is the *a priori estimation error* defined by

$$e(n) = d(n) - w^H(n-1)x(n) \quad (7.18)$$

The inner product  $w^H(n-1)x(n)$  represents an estimate of the desired response  $d(n)$ , based on the *old* least-squares estimate of the weight vector that was made at time  $n-1$ .

### 7.3 DIRECT SAMPLE COVARIANCE MATRIX INVERSION

One way to speed up the convergence rate is to employ the direct inversion of the covariance matrix  $R$  in (6.8) [16]. If the desired and interference signals are known a priori, then the covariance matrix could be evaluated and the optimal solution for the weights could be computed using (6.8), which requires direct SMI. In practice, the signals are not known and the signal environment undergoes frequent changes. Thus, the adaptive processor must continually update the weight vector to meet the requirements imposed by the varying conditions. This need to update the weight vector without a priori information leads to the expedient of obtaining estimates of  $R$  and  $r$  in

a finite observation interval and then using these estimates in (6.8) to obtain the desired weight vector. The estimates of both  $R$  and  $r$  can be evaluated, respectively, as

$$\hat{R} = \sum_{i=N_1}^{N_2} x(i)x^H(i) \quad (7.19)$$

and

$$\hat{r} = \sum_{i=N_1}^{N_2} d(i)x(i) \quad (7.20)$$

where  $N_1$  and  $N_2$  are the lower and upper limits of the observation interval or window, respectively. It follows from (6.8) that the estimate of the weight vector is given by,

$$\hat{w} = \hat{R}^{-1}\hat{r} \quad (7.21)$$

If we introduce a term represent the errors due to the estimates, we may write

$$e = \hat{R}w_{opt} - \hat{r} \quad (7.22)$$

which can be viewed as the least squares formulation of the problem.

## 7.4 SIMULATION RESULTS

In this section, some simulation results for Bit error rate (BER) and array patterns with single and two interfering signals cases will be illustrated. Output mean-square error (MSE) of adaptive antenna system will also be shown. Results are shown for BPSK, DPSK and NCFSK modulated signals. The Monte Carlo simulation is used to determine the BER performance of the adaptive antenna system. The simulation used  $10^5$  samples for a BER of  $10^{-4}$ .

In Figure 7.1, the average Bit error rate (BER) against the received SINR (signal-to-interference-plus-noise ratio) for adaptive antennas with one interferer and BPSK modulation is shown. The improvement in BER is mostly depend on  $\mu$  and  $\Gamma_1$ . If there is no interference (i.e,  $\Gamma_1=0$ ), the system will behave as a maximal ratio combiner. One can observe that the improvement in terms of the received SINR required for a given value of BER is nearly independent of the SINR for  $\text{BER} < 10^{-2}$ .

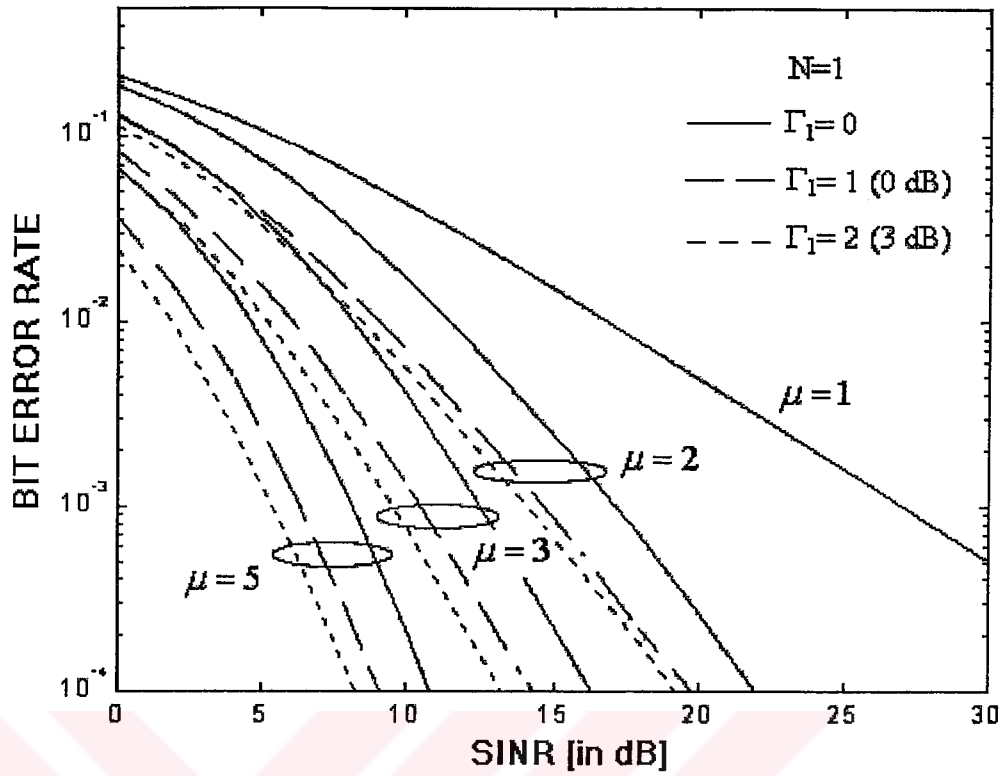
When there is more than one interferer and BPSK modulation, the BER results are shown in Figure 7.2. The improvement obtained using adaptive antennas increases with the number of antenna elements. For example, for  $\text{BER}=10^{-3}$  and  $\mu=5$ , adaptive antennas requires approximately 4.2 dB less than maximal ratio combining.

Figure 7.3 shows the BER against the average received SINR for adaptive antennas with a single interferer and DPSK modulation. Again, the results for  $\Gamma_1=0$  corresponds to those for maximal ratio combining. One can observe that the improvement in terms of the received SINR required for a given value of BER is almost independent of the SINR for  $\text{BER} < 10^{-2}$ .

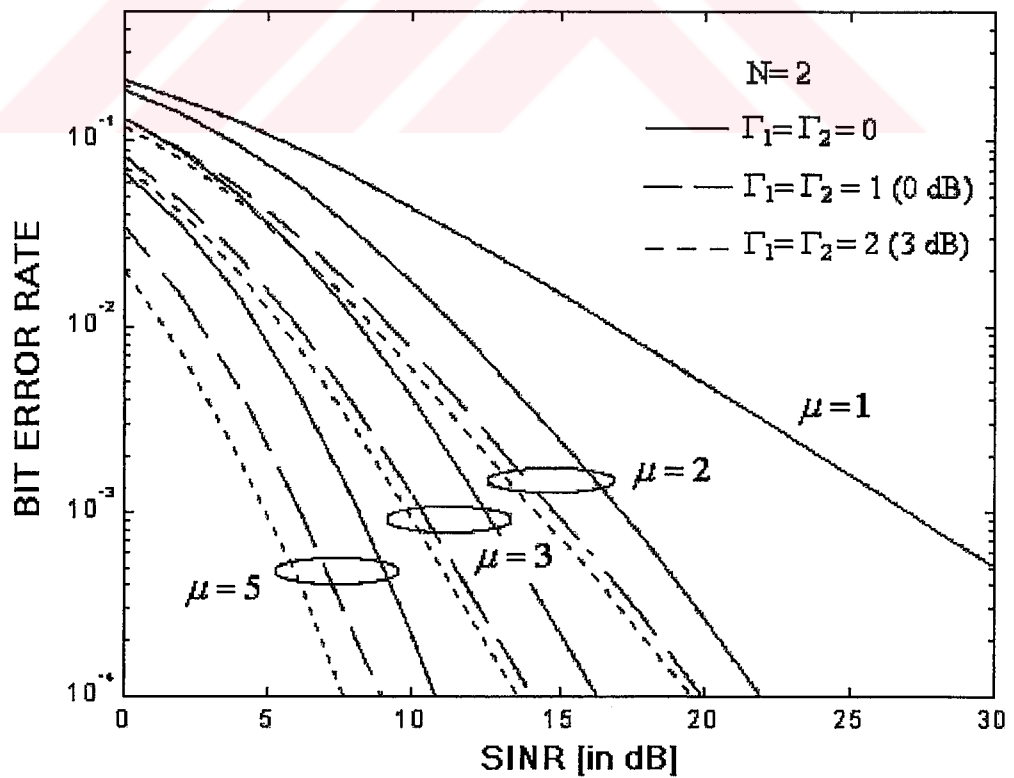
For two interferers and DPSK modulation, the BER results are shown in Figure 7.4. Again, the improvement obtained using adaptive antennas increases with the number of antenna elements. For DPSK modulated signals there is also a marked improvement as the number of antennas increases similar to BPSK modulation in Figure 7.1 and Figure 7.2. As seen, DPSK modulation is several decibels worse than BPSK modulation.

Figure 7.5 shows the BER against the average received SINR for adaptive antennas with a single interferer and NCFSK modulation. Again, the results for  $\Gamma_1=0$  corresponds to those for maximal ratio combining. One can observe that the improvement in terms of the received SINR required for a given value of BER is almost independent of the SINR for  $BER < 10^{-2}$ .

For two interferers and NCFSK modulation, the BER results are shown in Figure 7.6. Again, the improvement obtained using adaptive antennas increases with the number of antenna elements. For NCFSK modulated signals there is also a marked improvement as the number of antennas increases similar to DPSK modulation in Figure 7.3 and Figure 7.4. As seen, NCFSK modulation is several decibels worse than DPSK modulation.



**Figure 7.1** The average BER against the received SINR for adaptive antennas with one interferer and BPSK modulation. Results are shown for several values of  $\mu$  and  $\Gamma_1$ .



**Figure 7.2** The average BER against the received SINR for adaptive antennas with two equal power interferers and BPSK modulation.

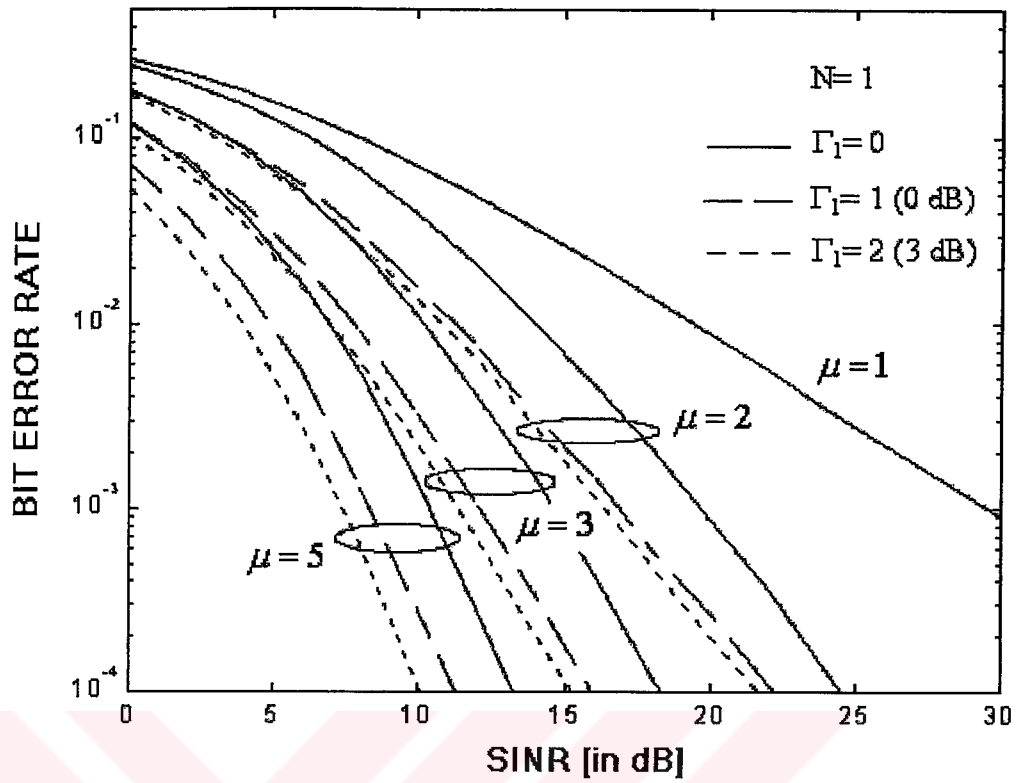


**Figure 7.3** The average BER against the received SINR for adaptive antennas with one interferer and DPSK modulation. Results are shown for several values of  $\mu$  and  $\Gamma_1$ .

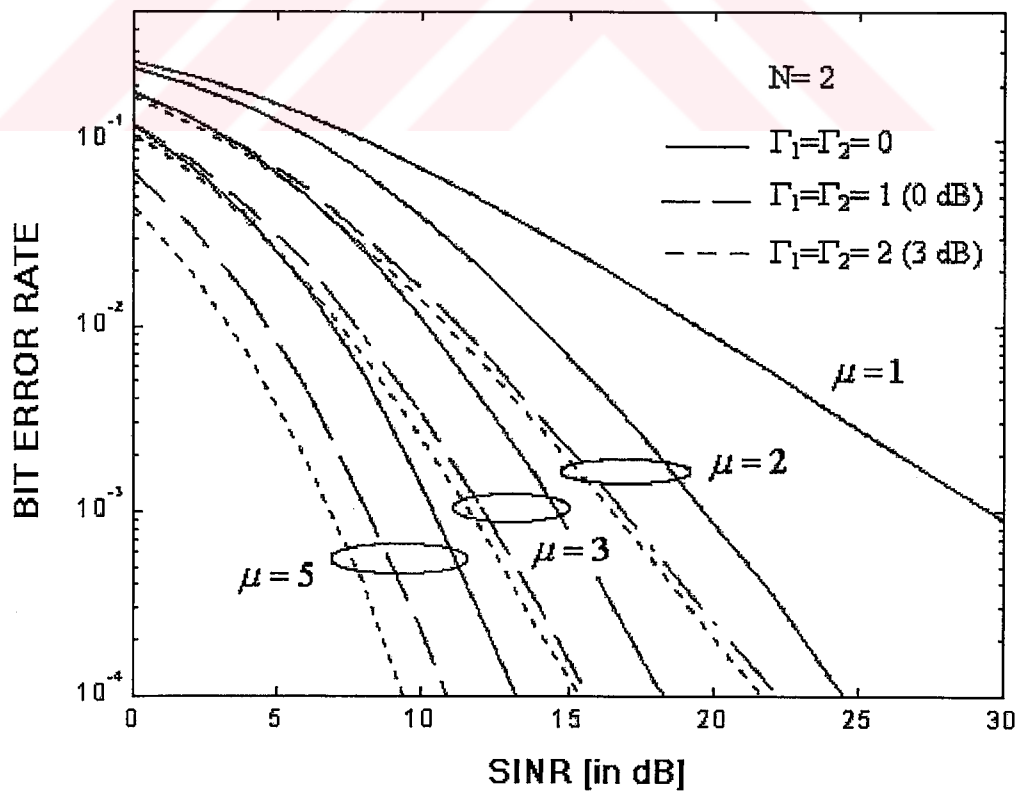


**Figure 7.4** The average BER against the received SINR for adaptive antennas with two equal power interferers and DPSK modulation.

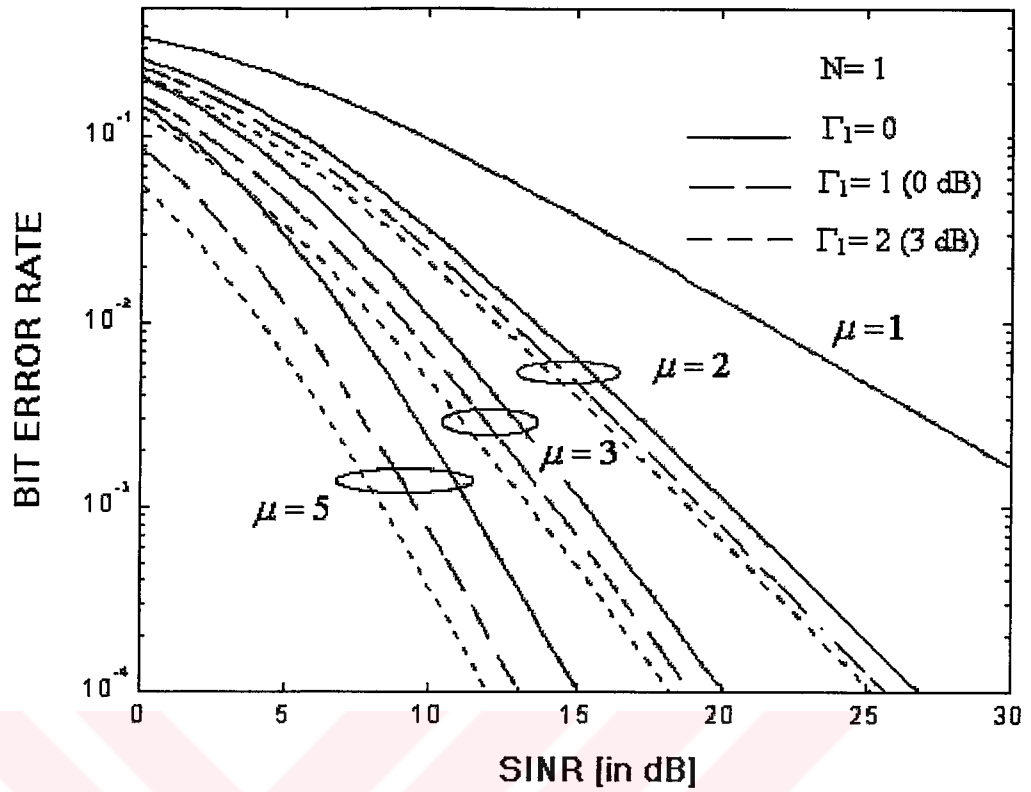


**Figure 7.5** The average BER against the received SINR for adaptive antennas with one interferer and NCFSK modulation. Results are shown for several values of  $\mu$  and  $\Gamma_1$ .

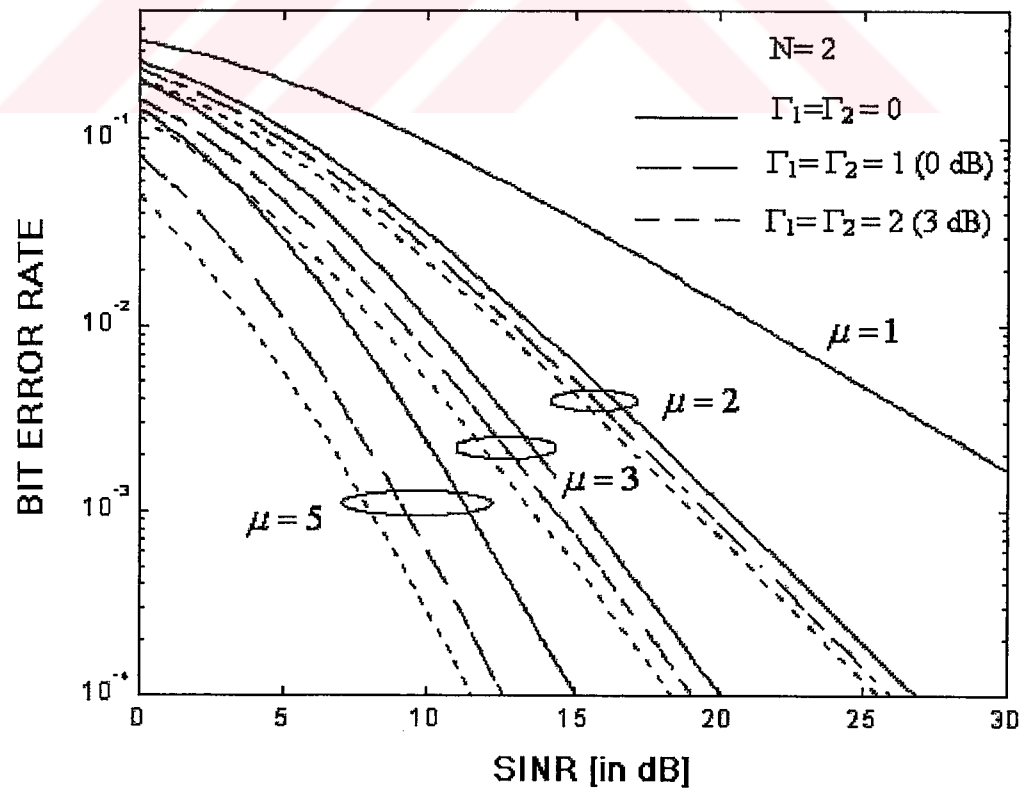


**Figure 7.6** The average BER against the received SINR for adaptive antennas with two equal power interferers and NCFSK modulation.

In Figure 7.7, the output MSE of adaptive antenna system for LMS algorithm is illustrated. As you can see, within the margin given by equation (7.9), the larger the value of  $\alpha$ , the faster the convergence but the less stability around the minimum value. On the other hand, the smaller the value of  $\alpha$ , the slower the convergence but the algorithm will be more stable around the optimum value.

In Figure 7.8, the output MSE of adaptive antenna system for LMS and RLS algorithms are illustrated on the same window. One can see that, RLS algorithm converges to optimum weights faster than LMS algorithm. RLS algorithm converges to optimum weights at about 100 iterations, on the other hand LMS algorithm converges at about 700 iterations.

In Figure 7.9, the output MSE of adaptive antenna system for DMI algorithm is shown. MSE is much less than the other algorithms LMS and RLS.

In Figure 7.10, the array patterns with LMS and RLS algorithms are illustrated for two interferers impinge upon the array at angles of  $\theta_1 = -30^\circ$  and  $\theta_2 = 45^\circ$  respectively. It is observed that, the system placed two nulls in the directions of interferers and steered towards the direction of interest,  $\theta_d = 0^\circ$ . The RLS algorithm has deeper nulls than LMS algorithm; this means RLS algorithm reduces interferences better than the LMS algorithm.

In Figure 7.11, the array patterns with LMS and DMI algorithms are illustrated for two interferers impinge upon the array at angles of  $\theta_1 = -30^\circ$  and  $\theta_2 = 45^\circ$  respectively. The DMI algorithm has deeper nulls than LMS algorithm.

In Figure 7.12, the array patterns with RLS and DMI algorithms are illustrated for two interferers impinge upon the array at angles of  $\theta_1 = -30^\circ$  and  $\theta_2 = 45^\circ$  respectively. The DMI algorithm has deeper nulls than RLS algorithm.



In Figure 7.13, the array pattern of adaptive antenna system for  $\theta_a = 90^\circ$  is illustrated. Also shown in this figure, when the desired angle is  $90^\circ$  or close to  $90^\circ$ , the nulls are formed in a well manner in the directions of interferers but the beam in desired direction could not be formed. The linear array in adaptive antenna system is unable to form narrow beams for impinging angles close to  $90^\circ$  s.

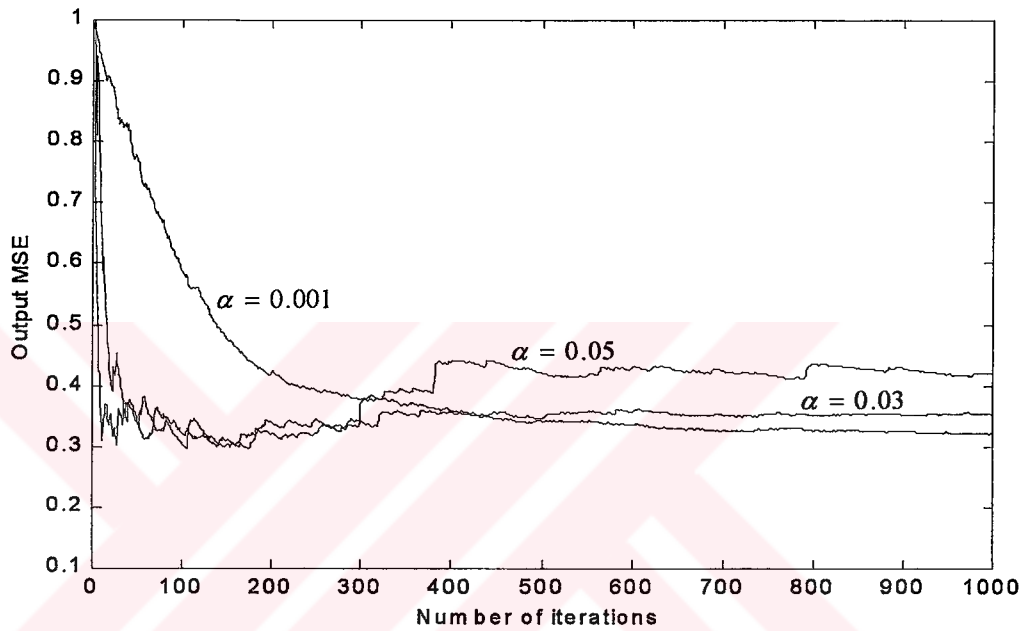


**Figure 7.7** The output MSE of adaptive antenna system for LMS algorithm with varying step size parameter  $\alpha$ .

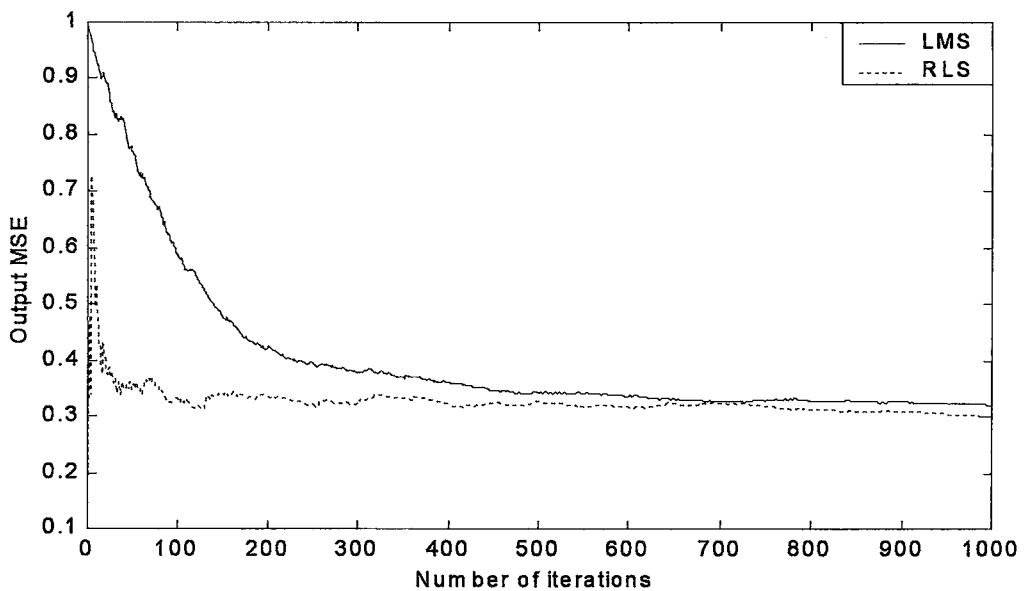


**Figure 7.8** The output MSE of adaptive antenna system for LMS and RLS algorithms.

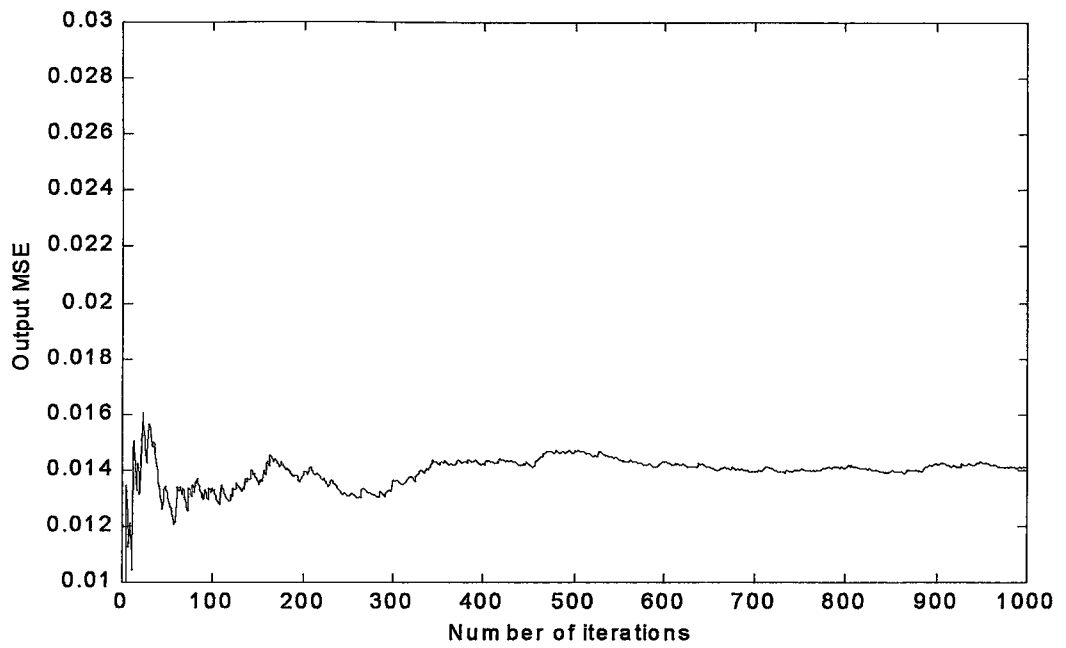


**Figure 7.9** The output MSE of adaptive antenna system for DMI algorithm .

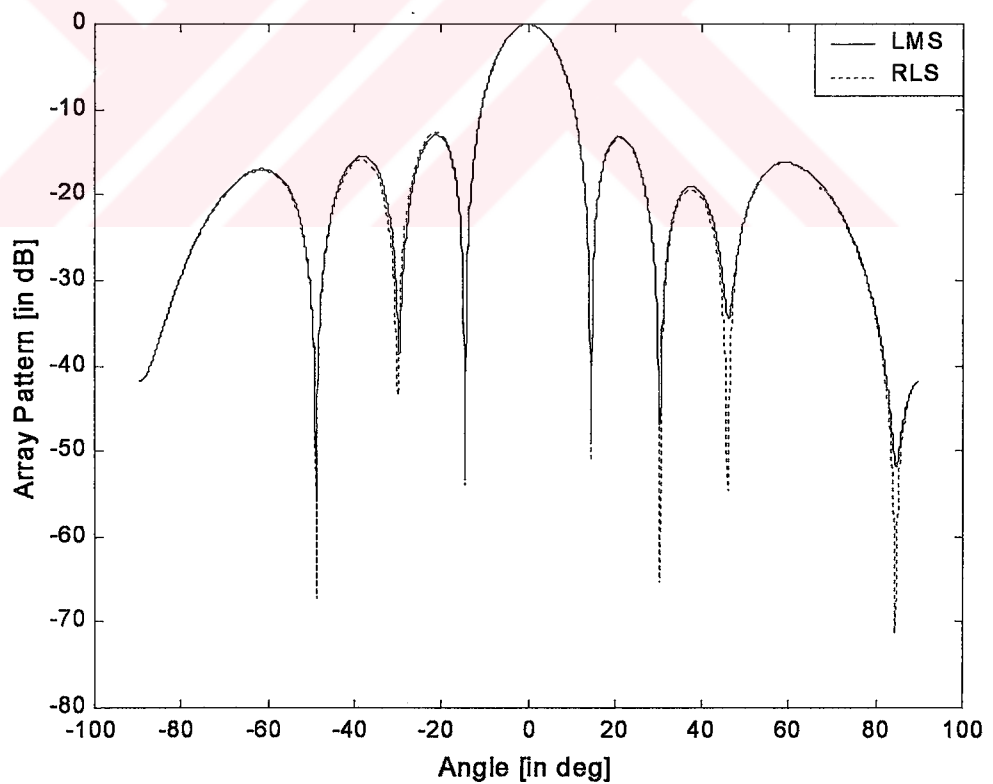


**Figure 7.10** Array patterns of adaptive antenna system for LMS and RLS algorithms with two interferers,  $N = 2$ .

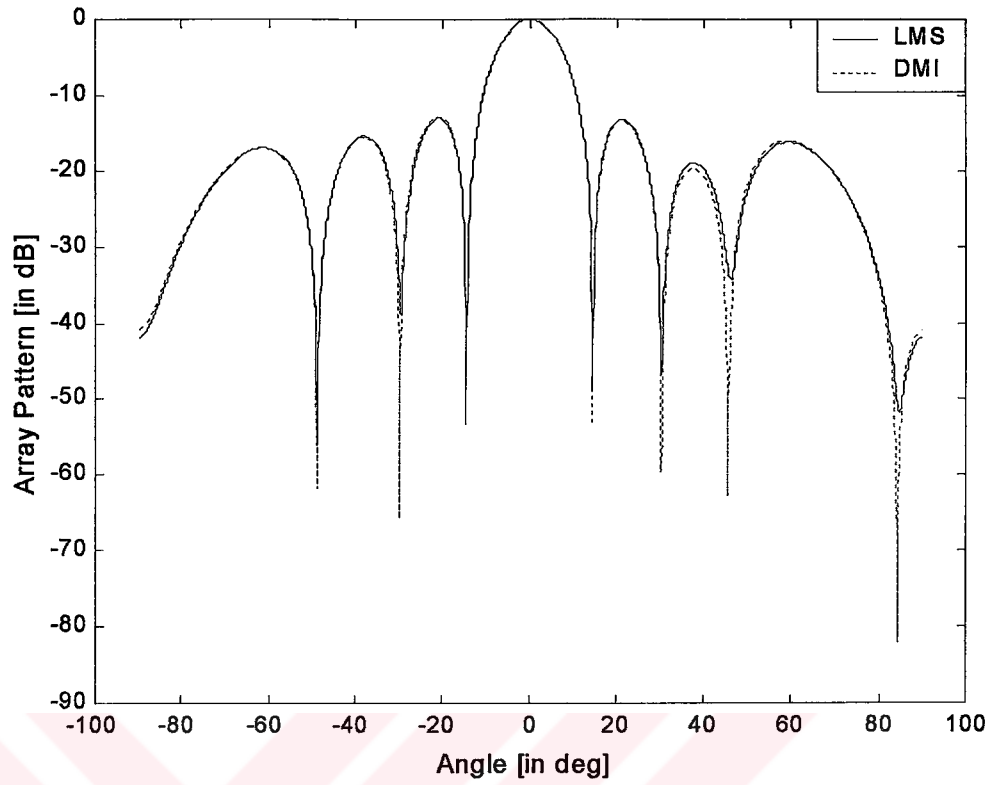


**Figure 7.11** Array patterns of adaptive antenna system for LMS and DMI algorithms with two interferers,  $N = 2$ .

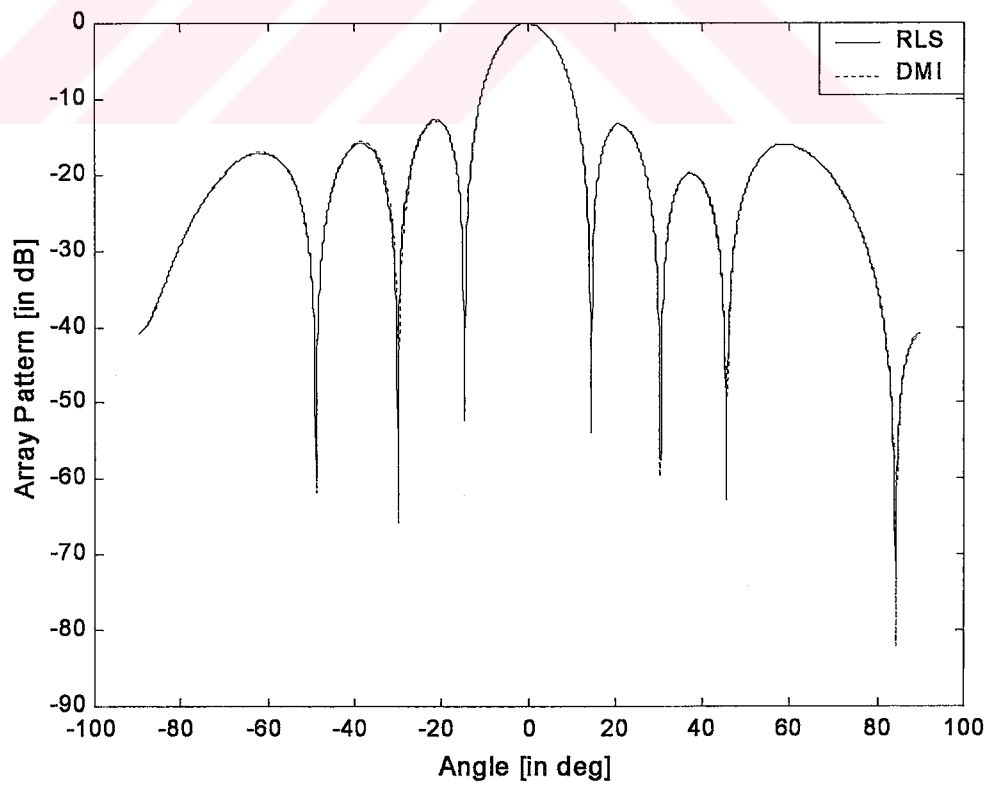


**Figure 7.12** Array patterns of adaptive antenna system for RLS and DMI algorithms with two interferers,  $N = 2$ .

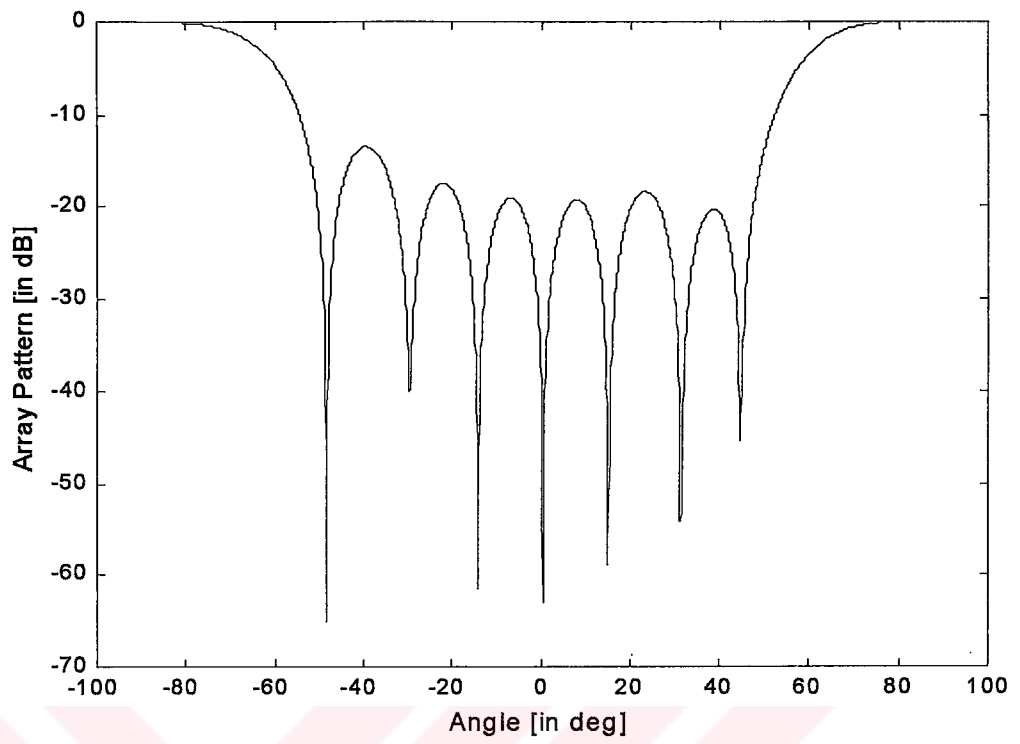


**Figure 7.13** Array pattern of adaptive antenna system with  $\theta_d = 90$ .

## CHAPTER 8

### CONCLUSIONS

In this thesis, we have investigated the benefit of the adaptive beamforming approach for wireless communication networks. A comparison made between the diversity systems and adaptive schemes has shown that a marked improvement in BER performance and capacity can be obtained.

The performance of selection combining and maximal ratio combining systems operating in a Rayleigh/Rician faded and lognormal shadowed environment has been studied. The average BER using BPSK, DPSK and NCFSK modulations in a Rayleigh/Rician faded and lognormal shadowed channels was derived.

It was observed that maximal ratio combining is seen to give larger improvement than selection combining in error performance. The largest diversity gain is achieved with 2-branch diversity and diminishing returns are realized with increasing  $L$ .

In general, the relative advantage of diversity is greater for Rayleigh fading than Rician fading, because as the Rice factor  $K_d$  increases there is less difference between the instantaneous received signal-to-noise ratios on the various diversity branches. However, the performance will always be better with Rician fading than with Rayleigh fading, for a given average received signal-to-noise ratio and diversity order.

It is apparent that selection combining results in the worst performance, followed by equal-gain. Once again, maximal ratio combining is seen to give best performance.

The aim of this thesis was the investigation of adaptive beamforming approach as a solution to improve the performance and the capacity of the wireless communication systems. In this context, an adaptive beamformer with ULA geometry is studied and its

performance is tested by computer simulations. We also describe techniques for implementing adaptive beamforming with the Least Mean Squares (LMS), Recursive Least Squares (RLS) and, Direct Sample Covariance Matrix Inversion (DMI) adaptive arrays. The DMI approach can be shown to converge more rapidly than the LMS algorithm, the practical difficulties that are associated with the DMI algorithm approach should be appreciated. It has two major problems : (1) increased computational complexity that can not be easily overcome through the use of VLSI, and (2) numerical instability resulting from the use of finite-precision arithmetic and the requirement of inverting a large matrix.

It was observed that the improvement in BER is mostly dependent on interference-to-noise ratio  $\Gamma$  and the number of antenna elements  $\mu$ . If there is no interference (i.e.,  $\Gamma=0$ ) the system will behave as a maximal ratio combiner. Adaptive beamforming with a strong interferer ( $\Gamma \rightarrow \infty$ ) gives the same results as maximal ratio combining without interference and with one less antenna element.

It was observed that the improvement in terms of the received SINR required for a given value of BER is nearly independent of the SINR for  $BER < 10^{-2}$ . The improvement obtained using adaptive beamforming schemes increases with the number of antenna elements. For example, for  $BER=10^{-3}$  and  $\mu= 5$ , adaptive beamforming schemes requires approximately 4.2 dB less than maximal ratio combining.

We can conclude that with the adaptive antenna technology, many of the system parameters that are considered constraints in a single-antenna system become parameters that a system designer has at his disposal to further optimize system performance. It is this aspect of adaptive antenna technology which is perhaps most attractive with regard to its inclusion in the next generation of wireless systems to be implemented.

## APPENDIX A

The BER in cellular radio systems is given by:

$$P_e = \sum_{n=1}^6 \binom{6}{n} P_n(e|n) a_c^n (1 - a_c)^{6-n} \quad (\text{A.1})$$

where  $n$  denotes the number of active co-channel interferers and  $a_c$  stands for the carried traffic per channel in erlang. The BER,  $P_n(e|n)$ , conditioned on the presence of  $n$  active co-channel interferers in a pure Rician fading environment for non-coherent DPSK and BPSK, is given by:

$$P_n(e|n) = \frac{1}{2(1+R)} e^{\left(\frac{K_d R}{1+R}\right)} \quad (\text{A.2})$$

where  $R$  is defined by:

$$R = \frac{P_{0d} T_b}{A P_{0u} T_b + B N_0} = \frac{1}{1 + K_d} \left[ \frac{1}{\frac{A}{P_{0d}/P_{0u}} + \frac{B}{E_b/N_0}} \right] \quad (\text{A.3})$$

For non-coherent DPSK;  $A=B=1$ , for BPSK;  $A=B=2$ . Here,  $E_b / N_0$  denotes the ratio of the local-mean energy per bit of the desired signal to noise density.

$$\frac{E_b}{N_0} = \frac{P_{0d} T_b}{N_0} \quad (\text{A.4})$$

Assuming that the desired signal and  $n$  individual co-channel interferers have the same transmitted power, the ratio of the received local-mean power levels of the desired signal and cumulative co-channel interference is found as;

$$\frac{P_{0d}}{P_{0u}} = \frac{1}{n} R_u^a \left( \frac{G + R_u}{G + 1} \right)^b \quad (\text{A.5})$$

where  $R_u = D / R$  and  $G = g / R$  denote, respectively, the frequency reuse distance and the turning point, both normalized with respect to the cell radius.

The conditional BER, for Rician faded desired signal with shadowed LOS component, may be written as:

$$P_n(e|n) = \frac{1}{2\sqrt{2\pi}(1+R)} \int_{-\infty}^{\infty} e^{-\frac{t^2}{2}} e^{-\frac{K_d'R}{1+R} e^{\sigma_{sd}t}} dt \quad (\text{A.6})$$

where

$$K_d' = \frac{e^{m_{sd}}}{P_{od}'} \quad (\text{A.7})$$

The conditional BER for signals undergoing correlated shadowing may be written as:

$$P_n(e|n) = \int_{-\infty}^{\infty} \int_{-\infty}^{\infty} \frac{1}{2(1+R)} e^{-\left(\frac{K_d'R}{1+R}\right)} f_{P_{od}, P_{ou}}(P_{od}, P_{ou}) dP_{od} dP_{ou} \quad (\text{A.8})$$

A variable transformation between  $P_{od}$  and  $\tau_d$  and between  $P_{ou}$  and  $\tau_u$  followed by another transformation with  $x=\tau_d$  and  $y=(\tau_u-\rho_{d,u}\tau_d)/(1-\rho_{d,u}^2)^{1/2}$  leads to the following expression for the conditional BER:

$$P_e(e|n) = \frac{1}{4\pi} \int_{-\infty}^{\infty} \int_{-\infty}^{\infty} e^{-(x^2+y^2)} \frac{e^{-\frac{K_d'R}{1+R}}}{1+R} dx dy \quad (\text{A.9})$$

Here,  $R$  is still given by (A.3) with the exception that,  $P_{od}$  and  $P_{ou}$  are now random with area mean powers  $\xi_d$  and  $\xi_u$ . The shadowed version of  $E_b / N_0$  may be written as:

$$\frac{E_b}{N_0} = \frac{T_b \xi_d}{N_0} e^{\sigma_{dx}} \quad (\text{A.10})$$



Similarly, the shadowed version of  $P_{od} / P_{ou}$  is given by:

$$\frac{P_{od}}{P_{ou}} = \left( \frac{G+R_u}{G+1} \right)^b R_u^a e^{(m_d - m_u + (\sigma_d - \sigma_u \rho_{d,u})x - \sigma_u \sqrt{1 - \rho_{d,u}^2} y)} \quad (\text{A.11})$$

Here,  $m_d = \ln(\xi_d)$  and  $\sigma_d$  denote, respectively, the logarithmic mean and the shadow spread of the desired signal while  $m_u = \ln(\xi_u)$  and  $\sigma_u$  are the corresponding parameters for the sum of  $n$  correlated co-channel interferers. Here,

$$x = \tau_d = \ln(P_{od} / \xi_d) / \sigma_d \quad (\text{A.12})$$

$$y = (\tau_u - \rho_{d,u} \tau_u) / (1 - \rho_{d,u}^2)^{1/2} \quad (\text{A.13})$$

$$\tau_u = \ln(P_{od} / \xi_u) / \sigma_u \quad (\text{A.14})$$

## REFERENCES

- [1] S. Haykin, "Communication Systems", 3<sup>rd</sup> Edition, John Wiley & Sons, 1994.
- [2] S. Haykin, "Adaptive Filter Theory", 3<sup>rd</sup> Edition, Prentice Hall, New Jersey, 1996.
- [3] J.G. Proakis, "Digital Communications", 3<sup>rd</sup> Edition, McGraw-Hill, New York, 1995.
- [4] Theodore S. Rappaport, "Wireless Communications, Principles and Practice", 2<sup>nd</sup> Edition, Prentice Hall, 2002.
- [5] R. T. Compton, R. J. Huff, W. G. Swarner, and A. A. Ksienski, "Adaptive arrays for communication systems: An overview of research at the Ohio State University", IEEE Trans. Antennas Propagat., vol. AP-24, pp. 599-607, 1976.
- [6] R. T. Compton, "An adaptive antenna in a spread spectrum communication system", Proc. IEEE, vol. 66, pp. 289-398, March 1978.
- [7] J. H. Winters, "Increased data rate for communication systems with adaptive antennas", in Proc. IEEE Int. Conf. Comm., June 1982.
- [8] Y. S. Yeh and D. O. Reudink, "Efficient spectrum utilization for mobile radio systems using space diversity", in IEE Int. Conf. Radio Spectrum Conservation Techniques, London, pp. 12-16, 1980.
- [9] Y. S. Yeh and D. O. Reudink, "Efficient spectrum utilization for mobile radio systems using space diversity", IEEE Trans. Comm., vol. COM-30, pp. 447-455, March 1982.
- [10] V. M. Bogachev and I. G. Kiselev, "Optimum combining of signals in space-diversity reception", Telecomm. Radio Eng., vol. 34/35, pp. 83-85, Oct. 1980.
- [11] M. J. Marcus and S. Das, "The potential use of adaptive antennas to increase land mobile frequency reuse", in IEEE Int. Conf. Radio Spectrum Conservation Techniques, University of Birmingham, U.K., pp. 113-117, 1983.
- [12] Jack H. Winters, "Optimum Combining in Digital Mobile Radio with Cochannel Interference", IEEE Transactions on Vehicular Technology, vol. vt-33, No. 3, August 1984.
- [13] John Litva, "Digital Beamforming in Wireless Communications", Artech House, 1996.
- [14] B. Widrow, P.E. Mantey, L.J. Griffiths, and B.B. Goode, "Adaptive antenna systems" Proc. IEEE, vol. 55, pp. 2143-2159, Dec. 1967.

- [15] W. Murray, "Numerical Methods for Unconstrained Optimization", Academic Press, New York, 1972.
- [16] I.S. Reed, J.D. Marlett, and L.E. Brennen, "Rapid convergence rate in adaptive arrays", IEEE Trans. Aerosp. Electron. Syst., vol. AES-10, pp. 853-863, Nov. 1974.
- [17] Jack H. Winters, "Optimum Combining for Indoor Radio Systems with Multiple Users", IEEE Transactions on Communications, vol. com-35, No. 11, November 1987.
- [18] Tien D. Pham, Keith G. Balmain, "Multipath Performance of Adaptive Antennas with Multiple Interferers and Correlated Fadings", IEEE Transactions on Vehicular Technology, vol. 48, No. 2, March 1999.
- [19] Simon C. Swales, Mark A. Beach, David J. Edwards, Joseph P. McGeehan, "The Performance Enhancement of Multibeam Adaptive Base-Station Antennas for Cellular Land Mobile Radio Systems", IEEE Transactions on Vehicular Technology, vol. 39, No. 1, February 1990.
- [20] Satoshi Tsukamoto, Takuji Sasoh, Takahiro Sasaki, "A Complex Baseband Platform for Spatial-Temporal Mobile Radio Channel Simulations", IEEE Transactions on Vehicular Technology, vol. 51, No. 6, November 2002.
- [21] W. F. Gabriel, "Adaptive arrays – an introduction", Proc. IEEE, vol. 64, pp. 239-272, February 1976.
- [22] J. H. Winters, "Signal acquisition and tracking with adaptive arrays in the digital mobile radio system IS-54 with flat fading", IEEE Trans. Veh. Technol., vol. 42, pp. 377-384, Nov. 1993.
- [23] A. Şafak, S. Bahadır, O. Çakır, "Adaptif Anten Dizilerini Kullanan Hücreli Sistemlerde Spektrum Verimliliği", SIU'2003, pp. 704-707, 18-20 June 2003, Koç University, Istanbul, Turkey.

## ÖZGEÇMİŞ

**Adı** : Oğuzhan **Soyadı** : Çakır  
**Uyruğu** : T.C. **Doğum Yeri** : Ankara  
**Doğum Tarihi** : 30 - 03 - 1978

**Görev Yeri** : Başkent Üniversitesi Elektrik-Elektronik Mühendisliği Bölümü  
**Görev Ünvanı** : Araştırma Görevlisi  
**İş Adresi** : Başkent Üniversitesi Elektrik-Elektronik Müh. Böl. Bağlıca Kampüsü  
Eskişehir Yolu 20. km, 06530 Etimesgut /Ankara.  
**İş Tel** : (0312) 234 10 10 dahili : 1458 **İş Fax** : (0312) 234 10 51  
**e-posta** : [ocakir@baskent.edu.tr](mailto:ocakir@baskent.edu.tr)

### İLK VE ORTA ÖĞRENİM DURUMU

Okul	İl / İlçe	Giriş	Çıkış	Mezuniyet Derecesi
Mustafa Kemal İlkokulu	Ankara / Balgat	1984	1989	Pekiyi
Bahçelievler Ortaokulu	Ankara / Emek	1989	1992	İyi
Yenimahalle Andolu Teknik Lisesi	Ankara / Yenimah.	1992	1996	İyi

### YÜKSEK ÖĞRENİM DURUMU

Üniversite	Ülke	Giriş	Çıkış	Ünvan	Derece
Başkent Üniversitesi	Türkiye	1996	2000	Lisans	2.76
Başkent Üniversitesi	Türkiye	2000	2003	Y. Lisans	3.42

### ÇALIŞTIĞI KURUMLAR

Kurum	İl / İlçe	Giriş	Çıkış	Görevi
Başkent Üniversitesi	Ankara / Etimesgut	2000	Devam	Arş. Grv.